A Melt Prepolymerization of Poly(ethylene Terephthalate) in Semibatch Stirred Reactors

G. D. LEI and K. Y. CHOI,* *Department of Chemical and Nuclear Engineering, University of Maryland, College Park, Maryland 20742*

Synopsis

A semibatch melt prepolymerization of poly(ethylene terephthalate) (PET) is studied. Being characterized by complex reaction pathways leading to various functional end groups and side products, PET prepolymerization process poses a challenging modeling problem. Ten distinct polymeric species have been defined in accordance with the type of functional end groups and the corresponding mass balance and moment equation are developed to estimate the progress of reaction and polymer molecular weight. The effect of various reactor operating conditions on the performance of the polymerization process has been examined through numerical simulation of the molecular species model developed. In particular, the effect of incomplete transesterification of methyl ester groups on the polymer molecular weight has been investigated in detail.

INTRODUCTION

Many industrial melt polycondensation processes are characterized by complex reaction pathways leading to high molecular weight polymers and various side products. Poly(ethylene terephthalate) (PET) is no exception. Although PET has been used for many years in manufacturing films and fibers, the improvement in PET quality control makes this polymer as one of the most versatile and important polymers useful for diversified applications (e.g., glass-reinforced PET as engineering plastics). Currently PET is produced on commercial scale by semibatch and continuous processes and for precise polymer quality control the latter is becoming more attractive.

The kinetics of melt polymerization of PET has been studied by many workers in the past and recent review by Ravindranath and Mashelkar[1,2] provides an excellent overview of our current understanding of reaction chemistry and process modeling. Their work indicates that the PET polymerization under industrial process conditions is more complicated than one may think. A multitude of polymerization pathways leading to propagation, degradation, and side reactions gives rise to many challenging problems for the precise control of polymer properties. Some side products have adverse influence on the polymer quality. For example, a small amount of diethylene glycol (DEG) lowers the melting point and the thermal stability of PET. A few ppm of acetaldehyde gives a flavor to PET bottles and causes coloring problem. Table I illustrates the qualitative effect of various side products on the properties of PET.[3] Thus, it will be important to have an adequate control of such unwanted side products during the polymerization. Obviously, very simple process models may not be

* To whom correspondence should be addressed.

Journal of Applied Polymer Science, Vol. 41, 2987–3024 (1990)
 CCC 0021-8995/90/11-122987-38$04.00

TABLE I
Influences of Side Products on PET Properties[3]

End groups and side products	Polymer properties										
	Temperature stability	Light stability	Melting point	Density	Unit cell parameters	Crystallinity	Susceptibility to hydrolysis	Polymerization rate	Discoloration	Viscosity	Dyeing ability
Diethylene glycol $HOC_2H_4OC_2H_4OH$	↘	↘	↘	↘	No effect	↘					↗
Carboxyl end groups ~~COOH							↗	↘			
Hydroxyl end groups ~~OH										↘	
Methyl end groups ~~$COOCH_3$										↘	
Vinyl end groups ~~$CH=CH_2$									↗		
Cyclic oligomers C_n						No effect					↘
Acetaldehyde CH_3CHO									↗		
Water H_2O	↘						↗			↘	

satisfactory in describing the progress of polymerization and the resulting polymer properties.

The modeling of PET polymerization has been studied extensively in recent years by two Indian research schools led by Ravindranath and Mashelkar[1,2,4–8] and Gupta and Kumar.[9–11] In their pioneering works, they identified various reactions occurring in the melt polycondensation process and proposed detailed reactor models for the elucidation of polymerization behavior. As pointed out by these workers, one of the difficulties one may face in developing a comprehensive reaction model is the fact that the kinetics of various side reactions have not been studied quantitatively in the past. This implies that any detailed process models describing the melt PET process are difficult to validate due to the lack of appropriate experimental data. Nevertheless, such detailed modeling works as performed by the previous authors provide deeper insight into the complex condensation polymerization process and is useful for the process improvement.

In this work, we shall extend the previous modeling effort of Ravindranath and Mashelkar[4] on semibatch prepolymerization. As will be shown later, almost all the possible reactions except cyclization reaction have been considered in our model. These reactions are: ester interchange reaction, transesterification, polycondensation, acid end group formation, free DEG formation, DEG end group formation, esterification, diester group degradation, polycondensation of DEG end group, and redistribution reactions. The model, although, in some sense, cumbersome to develop and solve, gives more information on the details of product composition, molecular weight distribution, and side product formation.

MODEL DEVELOPMENT

The major functional end groups present in the polymerization melt are hydroxyethyl group, methyl ester group, carboxyl acid group, and diethylene glycol group. Since the polymerization is conducted in bulk polymer melt at high temperature (260–300°C) and low pressure, various functional end groups such as hydroxyethyl group, carboxyl group, etc. are very reactive and therefore an extensive redistribution of functional groups occurs during the course of polymerization. When one attempts to develop a PET polymerization model, the first task is to determine what reactions should be included in the kinetic scheme. In the modeling work by Ravindranath and Mashelkar,[4,7] both the functional group modeling approach and the molecular species modeling approach were used. However, the kinetic schemes or reactions considered in the two modeling works were quite different. For example, in the functional group model,[4] Raoult's law was used for vapor–liquid equilibrium calculations and the following reactions were included in the kinetic scheme: ester interchange reaction, transesterification, polycondensation, DEG and acid group formation, esterification, and degradation, whereas in the molecular species model,[7] the Flory–Huggins model was used and the following reactions were included: polycondensation, esterification, degradation of ester linkages and hydroxyethyl end groups, intermolecular alcoholysis and intermolecular acidolysis. In the latter, DEG formation reaction was not included.

Taking into account all possible reactions between these functional end groups, one can define 10 distinct polymeric species according to the type of two end groups attached to the polymer chain ends. Table II shows these 10 polymeric species. Note that P_1 (bis-hydroxyethyl terephthalate or BHET), Q_1 (methyl-hydroxyethyl terephthalate or MHET), R_1 (dimethyl terephthalate or DMT), S_1 (hydroxyethyl terephthalic acid or HTPA), and U_1 (methyl terephthalic acid or MTPA) are the transesterification products transferred from the first stage reactor. Together with ethylene glycol (EG) they are the major initial constituents in the second stage (i.e., prepolymerization). When compared with the polymeric species included in the modeling work of Ravindranath and Mashelkar,[7] the polymeric species listed in Table II include more species such as those containing terminal methyl ester group (e.g., Q_n, R_n, U_n, V_n)

TABLE II
Chemical Formulae of Polymeric Species

P_n	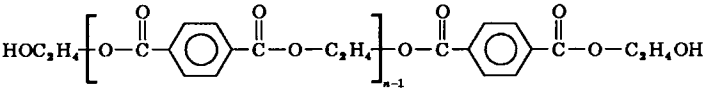
Q_n	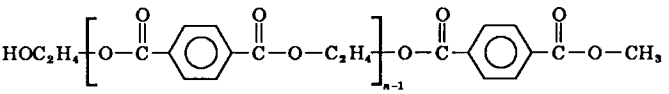
R_n	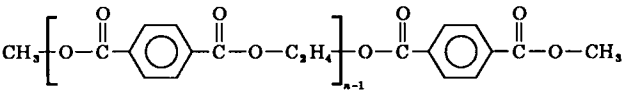
S_n	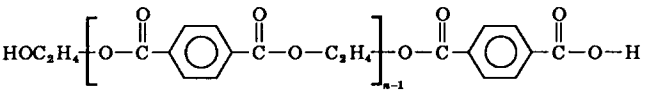
T_n	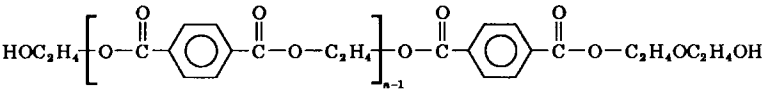
U_n	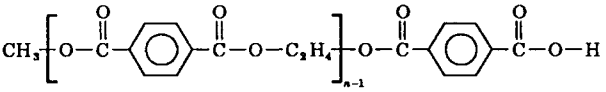
V_n	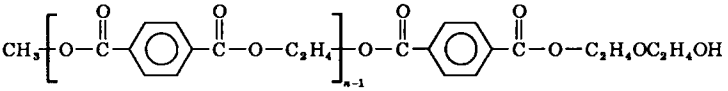
W_n	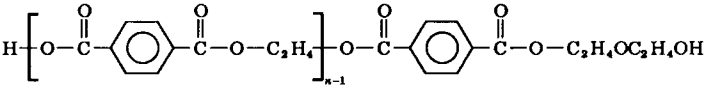
Y_n	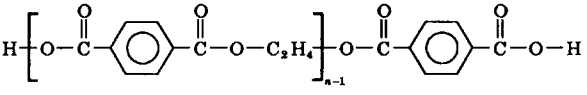
Z_n	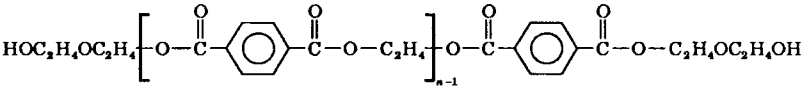

and diethylene glycol group (e.g., V_n, W_n, Z_n). The inclusion of such additional species significantly complicates the overall kinetic scheme; however, these species are indeed present in the polymerizing melt particularly when the prepolymerization starts with a mixture of completely transesterified DMT (i.e., BHET) and half-transesterified DMT (i.e., MHET). Moreover, the formation of free DEG and terminal DEG can also be predicted by using the proposed kinetic scheme. The reactions between the various functional groups are summarized in Table III. Although cyclic polymers (or oligomers) can also be formed, the amount of cyclic polymers is extremely small,[3,12] and thus the reactions leading to such cyclic polymers are not included in our reaction scheme. In Figure 1, the reaction network of melt polymerization of PET is summarized. This diagram shows complex reaction pathways considered in our subsequent kinetic modeling.

The main polycondensation reaction occurs in the presence of catalyst (e.g., Sb_2O_3) when two hydroxyethyl end groups react with each other to form a new ester linkage and to generate ethylene glycol as a condensation byproduct. The polycondensation reaction can be expressed as following (for $n, m \geq 1$):

$$P_n + P_m \underset{2(n+m-1)k_p'}{\overset{4k_p}{\rightleftharpoons}} P_{n+m} + EG \tag{1a}$$

$$P_n + Q_m \underset{2(n+m-1)k_p'}{\overset{2k_p}{\rightleftharpoons}} Q_{n+m} + EG \tag{1b}$$

$$P_n + S_m \underset{2(n+m-1)k_p'}{\overset{2k_p}{\rightleftharpoons}} S_{n+m} + EG \tag{1c}$$

$$P_n + T_m \underset{2(n+m-1)k_p'}{\overset{2k_p}{\rightleftharpoons}} T_{n+m} + EG \tag{1d}$$

$$Q_n + Q_m \underset{2(n+m-1)k_p'}{\overset{k_p}{\rightleftharpoons}} R_{n+m} + EG \tag{1e}$$

$$Q_n + S_m \underset{2(n+m-1)k_p'}{\overset{k_p}{\rightleftharpoons}} U_{n+m} + EG \tag{1f}$$

$$Q_n + T_m \underset{2(n+m-1)k_p'}{\overset{k_p}{\rightleftharpoons}} V_{n+m} + EG \tag{1g}$$

$$S_n + S_m \underset{2(n+m-1)k_p'}{\overset{k_p}{\rightleftharpoons}} Y_{n+m} + EG \tag{1h}$$

$$S_n + T_m \underset{2(n+m-1)k_p'}{\overset{k_p}{\rightleftharpoons}} W_{n+m} + EG \tag{1i}$$

$$T_n + T_m \underset{2(n+m-1)k_p'}{\overset{k_p}{\rightleftharpoons}} Z_{n+m} + EG \tag{1j}$$

where k_p is the forward polycondensation rate constant for the reaction of two hydroxyethyl end groups and k_p' the backward reaction rate constant for the reaction of the hydroxyl group in ethylene glycol with the ester linkage in the polymer chain, and EG the ethylene glycol. The multiple in front of each rate constant indicates the number of reaction sites available for the reaction.

To reduce the reaction time in the first stage, the transesterification reaction is generally carried out to 80–90% conversion of methyl ester group and unreacted methyl ester groups are then transferred to the second stage prepoly-

TABLE III
Various Reactions in Melt Polymerization of PET

Ester interchange:

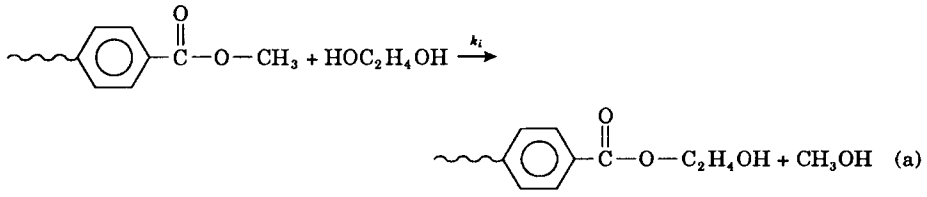

(a)

Transesterification:

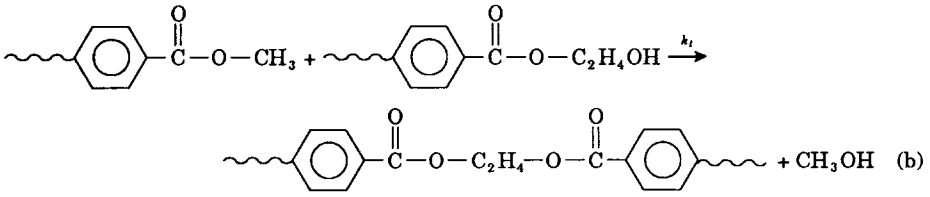

(b)

Polycondensation:

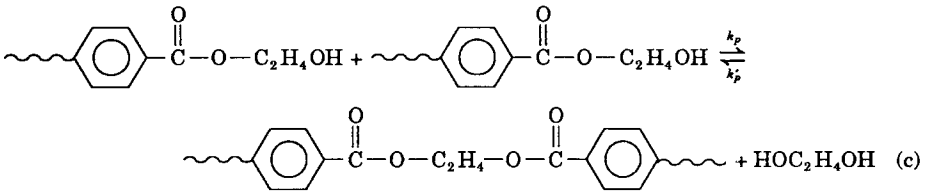

(c)

Acid end group formation:

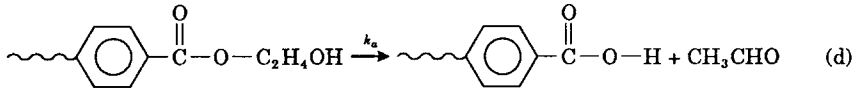

(d)

Free diethylene glycol formation:

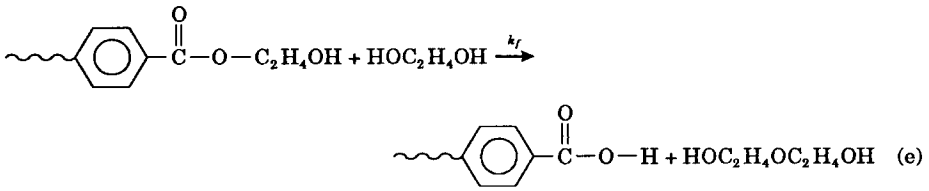

(e)

Diethylene glycol end group formation:

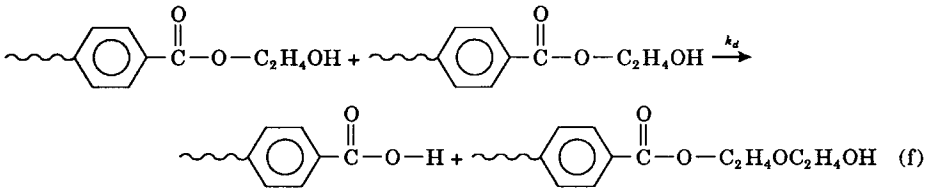

(f)

TABLE III *(Continued from the previous page.)*

Esterification:

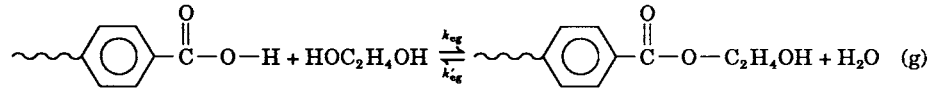

(g)

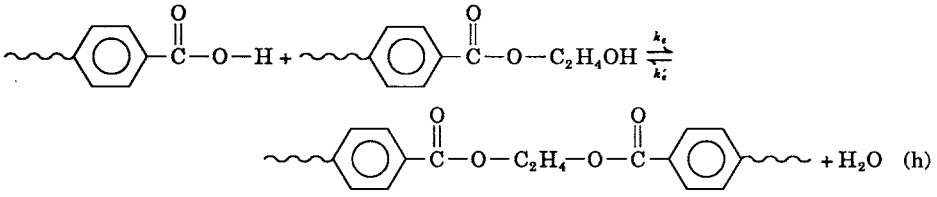

(h)

Degradation of diester group:

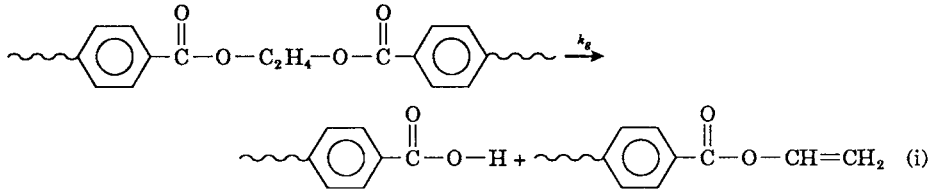

(i)

Polycondensation of diethylene glycol end group:

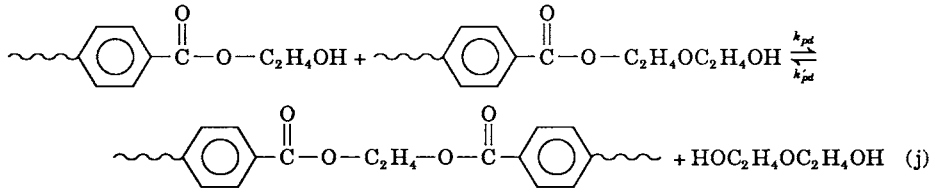

(j)

Redistribution reactions:

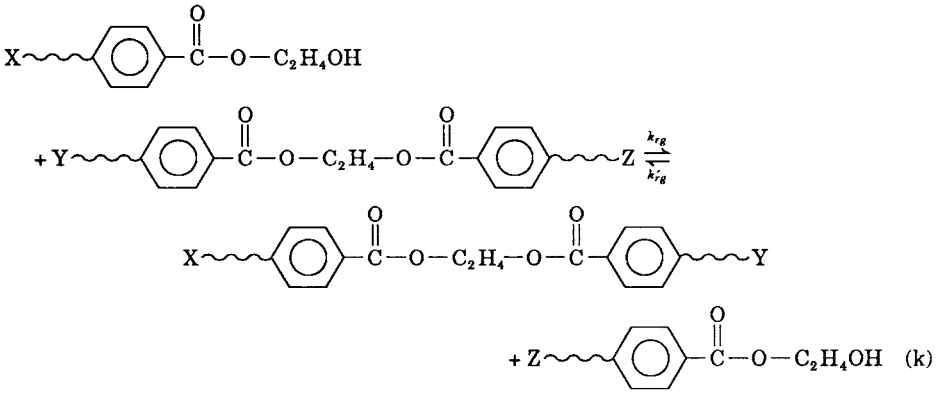

(k)

merization reactor in the form of MHET (Q_1) or DMT (R_1). Thus, the following transesterification and ester interchange reactions will also occur in the prepolymerization stage:

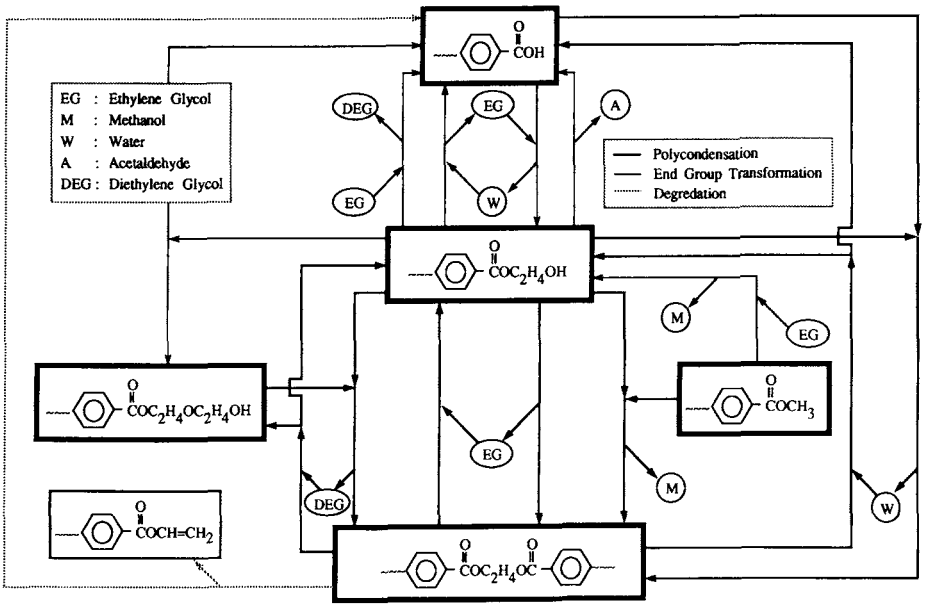

Fig. 1. Reaction network of melt polymerization of poly(ethylene terephthalate).

Transesterification reactions (for n, m ≥ 1):

$$P_n + Q_m \xrightarrow{2k_t} P_{n+m} + M \quad (2a)$$

$$P_n + R_m \xrightarrow{4k_t} Q_{n+m} + M \quad (2b)$$

$$P_n + U_m \xrightarrow{2k_t} S_{n+m} + M \quad (2c)$$

$$P_n + V_m \xrightarrow{2k_t} T_{n+m} + M \quad (2d)$$

$$Q_n + Q_m \xrightarrow{2k_t} Q_{n+m} + M \quad (2e)$$

$$Q_n + R_m \xrightarrow{2k_t} R_{n+m} + M \quad (2f)$$

$$Q_n + U_m \xrightarrow{k_t} U_{n+m} + M \quad (2g)$$

$$Q_n + V_m \xrightarrow{k_t} V_{n+m} + M \quad (2h)$$

$$S_n + Q_m \xrightarrow{k_t} S_{n+m} + M \quad (2i)$$

$$S_n + R_m \xrightarrow{2k_t} U_{n+m} + M \quad (2j)$$

$$S_n + U_m \xrightarrow{k_t} W_{n+m} + M \quad (2k)$$

$$S_n + V_m \xrightarrow{k_t} Y_{n+m} + M \quad (2l)$$

$$T_n + Q_m \xrightarrow{k_t} T_{n+m} + M \quad (2m)$$

$$T_n + R_m \xrightarrow{2k_t} V_{n+m} + M \quad (2n)$$

$$T_n + U_m \xrightarrow{k_t} W_{n+m} + M \quad (2o)$$

$$T_n + V_m \xrightarrow{k_t} Z_{n+m} + M \quad (2p)$$

Ester interchange reactions (for $n \geq 1$):

$$Q_n + EG \xrightarrow{2k_i} P_n + M \tag{3a}$$

$$R_n + EG \xrightarrow{4k_i} Q_n + M \tag{3b}$$

$$U_n + EG \xrightarrow{2k_i} S_n + M \tag{3c}$$

$$V_n + EG \xrightarrow{2k_i} T_n + M \tag{3d}$$

where k_t is the transesterification rate constant for the reaction of hydroxyethyl group with methyl ester group, k_i the ester interchange rate constant for the hydroxyl group in ethylene glycol with methyl ester group, and M represents methanol. Since the polycondensation reaction temperature (260–280°C) is above the critical temperature of methanol (239.5°C) and the polymerization reactor pressure is very low, it is reasonable to assume that methanol will vaporize as soon as it is formed. Then, only forward reactions are considered in both the transesterification and the ester interchange reactions.

As shown in Table III, carboxyl acid end groups are formed via several different reactions (d, e, f, i). The amount of carboxyl groups present in the polymer is an important factor in connection with their susceptibility to hydrolysis, since these end groups have a catalytic effect in the process.[13] The acid end group formation reactions are represented as follows (for $n \geq 1$):

$$P_n \xrightarrow{2k_a} S_n + A \tag{4a}$$

$$Q_n \xrightarrow{k_a} U_n + A \tag{4b}$$

$$S_n \xrightarrow{k_a} Y_n + A \tag{4c}$$

$$T_n \xrightarrow{k_a} W_n + A \tag{4d}$$

where k_a is the rate constant for the transformation reaction of hydroxyethyl end group to acid end group and acetaldehyde (A). The critical temperature of acetaldehyde (188°C) is much lower than the reaction temperature and we can assume that the concentration of acetaldehyde in the reaction mixture is negligible. However, acid end groups react with ethylene glycol to reproduce the hydroxyethyl end group and another side product, water. Such reactions are known as esterification reactions and they are, for $n \geq 1$,

$$S_n + EG \underset{2k'_{eg}}{\overset{2k_{eg}}{\rightleftharpoons}} P_n + W \tag{5a}$$

$$U_n + EG \underset{k'_{eg}}{\overset{2k_{eg}}{\rightleftharpoons}} Q_n + W \tag{5b}$$

$$W_n + EG \underset{k'_{eg}}{\overset{2k_{eg}}{\rightleftharpoons}} T_n + W \tag{5c}$$

$$Y_n + EG \underset{k'_{eg}}{\overset{4k_{eg}}{\rightleftharpoons}} S_n + W \tag{5d}$$

where k_{eg} is the forward rate constant for the reaction of acid end group with the hydroxyl group in ethylene glycol and k'_{eg} the reverse rate constant for the reaction of hydroxyethyl end group with water (W). Another type of esterifi-

cation reaction occurs when acid end group reacts with hydroxyethyl end group as shown in Table III [reaction (h)]. The molecular species model for this reaction can be expressed as (for $n, m \geq 1$)

$$P_n + S_m \underset{2(n+m-1)k_e'}{\overset{2k_e}{\rightleftharpoons}} P_{n+m} + W \tag{6a}$$

$$P_n + U_m \underset{(n+m-1)k_e'}{\overset{2k_e}{\rightleftharpoons}} Q_{n+m} + W \tag{6b}$$

$$P_n + W_m \underset{(n+m-1)k_e'}{\overset{2k_e}{\rightleftharpoons}} T_{n+m} + W \tag{6c}$$

$$P_n + Y_m \underset{(n+m-1)k_e'}{\overset{4k_e}{\rightleftharpoons}} S_{n+m} + W \tag{6d}$$

$$Q_n + S_m \underset{(n+m-1)k_e'}{\overset{k_e}{\rightleftharpoons}} Q_{n+m} + W \tag{6e}$$

$$Q_n + U_m \underset{2(n+m-1)k_e'}{\overset{k_e}{\rightleftharpoons}} R_{n+m} + W \tag{6f}$$

$$Q_n + W_m \underset{(n+m-1)k_e'}{\overset{k_e}{\rightleftharpoons}} V_{n+m} + W \tag{6g}$$

$$Q_n + Y_m \underset{(n+m-1)k_e'}{\overset{2k_e}{\rightleftharpoons}} U_{n+m} + W \tag{6h}$$

$$S_n + S_m \underset{(n+m-1)k_e'}{\overset{2k_e}{\rightleftharpoons}} S_{n+m} + W \tag{6i}$$

$$S_n + U_m \underset{(n+m-1)k_e'}{\overset{k_e}{\rightleftharpoons}} U_{n+m} + W \tag{6j}$$

$$S_n + W_m \underset{(n+m-1)k_e'}{\overset{k_e}{\rightleftharpoons}} W_{n+m} + W \tag{6k}$$

$$S_n + Y_m \underset{2(n+m-1)k_e'}{\overset{2k_e}{\rightleftharpoons}} Y_{n+m} + W \tag{6l}$$

$$T_n + S_m \underset{(n+m-1)k_e'}{\overset{k_e}{\rightleftharpoons}} T_{n+m} + W \tag{6m}$$

$$T_n + U_m \underset{(n+m-1)k_e'}{\overset{k_e}{\rightleftharpoons}} V_{n+m} + W \tag{6n}$$

$$T_n + W_m \underset{2(n+m-1)k_e'}{\overset{k_e}{\rightleftharpoons}} Z_{n+m} + W \tag{6o}$$

$$T_n + Y_m \underset{(n+m-1)k_e'}{\overset{2k_e}{\rightleftharpoons}} W_{n+m} + W \tag{6p}$$

where k_e is the forward esterification rate constant for the reaction of acid end group with hydroxyethyl end group and k_e' the reverse esterification rate constant for the reaction of water with the diester group in the polymer chain. Note that, depending upon which side of a diester group in the polymer reacts with a water molecule, different species can be produced from the same reactant in some of the reverse reactions. For example, if water reacts with the hydroxyethyl end group side of any diester group in species Q, the end products will be Q and S as in eq. (6e). However, P and U will be the products if water reacts with the methyl ester end group side of a diester group in species Q, as in eq. (6b).

Every 1 wt % of diethylene glycol in PET can lower the melting point by 5°C. However, an increased amount of DEG increases the dyeability of PET.[3]

Therefore, it is important to keep the DEG content in the polymer within certain limits. In our molecular species model, DEG was considered both as a volatile species when it is free in the polymer melt and as a polymeric species when it is incorporated into the polymer chain end. The reactions leading to DEG are shown in Table III [reactions (e, f)]. The molecular species model for this reaction can be expressed as (for $n \geq 1$):

$$P_n + EG \xrightarrow{4k_f} S_n + DEG \tag{7a}$$

$$Q_n + EG \xrightarrow{2k_f} U_n + DEG \tag{7b}$$

$$S_n + EG \xrightarrow{2k_f} Y_n + DEG \tag{7c}$$

$$T_n + EG \xrightarrow{2k_f} W_n + DEG \tag{7d}$$

where k_f is the rate constant for the reaction of hydroxyethyl end group with the hydroxyl group in ethylene glycol. Free DEG can also be produced by the dehydration reaction of ethylene glycols. However, Yoda[14] reported that this reaction route to DEG is not significant with Sb_2O_3 catalyst (e.g., $< 1.0 \times 10^{-4}$ wt % of EG). The polymers with DEG end groups are formed by the following reactions (for $n, m \geq 1$):

$$P_n + P_m \xrightarrow{8k_d} S_n + T_m \tag{8a}$$

$$P_n + Q_m \xrightarrow{2k_d} S_n + V_m \tag{8b}$$

$$P_n + Q_m \xrightarrow{2k_d} T_n + U_m \tag{8c}$$

$$P_n + S_m \xrightarrow{2k_d} S_n + W_m \tag{8d}$$

$$P_n + S_m \xrightarrow{2k_d} T_n + Y_m \tag{8e}$$

$$P_n + T_m \xrightarrow{2k_d} S_n + Z_m \tag{8f}$$

$$P_n + T_m \xrightarrow{2k_d} T_n + W_m \tag{8g}$$

$$Q_n + Q_m \xrightarrow{2k_d} U_n + V_m \tag{8h}$$

$$Q_n + S_m \xrightarrow{k_d} U_n + W_m \tag{8i}$$

$$Q_n + S_m \xrightarrow{k_d} V_n + Y_m \tag{8j}$$

$$Q_n + T_m \xrightarrow{k_d} U_n + Z_m \tag{8k}$$

$$Q_n + T_m \xrightarrow{k_d} V_n + W_m \tag{8l}$$

$$S_n + S_m \xrightarrow{2k_d} W_n + Y_m \tag{8m}$$

$$S_n + T_m \xrightarrow{k_d} W_n + W_m \tag{8n}$$

$$S_n + T_m \xrightarrow{k_d} Y_n + Z_m \tag{8o}$$

$$T_n + T_m \xrightarrow{2k_d} W_n + Z_m \tag{8p}$$

where k_d is the rate constant for the reaction of two hydroxyethyl end groups leading to the formation of diethylene glycol end group and acid end group. If

we consider these reactions as bidirectional transfer of one hydroxyethyl end group between the two polymeric species, it is easy to realize why there are two sets of products produced from the same set of reactants in some of these reactions, e.g., eqs. (8i) and (8j). Note that different multiplicity factors in front of the rate constants in the above reaction schemes represent all the possible reaction pathways of the two polymeric species involved in the reactions.

Since diethylene glycol end groups can also be considered as another kind of hydroxyethyl end groups having an ether linkage at the end, it is reasonable to assume that DEG end groups will be involved in the polycondensation reactions just like hydroxyethyl end groups. Then, the molecular species model for those reactions leading to DEG can be expressed as (for $n, m \geq 1$):

$$P_n + T_m \underset{4(n+m-1)k'_{pd}}{\overset{2k_{pd}}{\rightleftharpoons}} P_{n+m} + DEG \tag{9a}$$

$$Q_n + T_m \underset{2(n+m-1)k'_{pd}}{\overset{k_{pd}}{\rightleftharpoons}} Q_{n+m} + DEG \tag{9b}$$

$$S_n + T_m \underset{2(n+m-1)k'_{pd}}{\overset{k_{pd}}{\rightleftharpoons}} S_{n+m} + DEG \tag{9c}$$

$$T_n + T_m \underset{2(n+m-1)k'_{pd}}{\overset{2k_{pd}}{\rightleftharpoons}} T_{n+m} + DEG \tag{9d}$$

$$P_n + V_m \underset{2(n+m-1)k'_{pd}}{\overset{2k_{pd}}{\rightleftharpoons}} Q_{n+m} + DEG \tag{9e}$$

$$Q_n + V_m \underset{4(n+m-1)k'_{pd}}{\overset{k_{pd}}{\rightleftharpoons}} R_{n+m} + DEG \tag{9f}$$

$$S_n + V_m \underset{2(n+m-1)k'_{pd}}{\overset{k_{pd}}{\rightleftharpoons}} U_{n+m} + DEG \tag{9g}$$

$$T_n + V_m \underset{2(n+m-1)k'_{pd}}{\overset{k_{pd}}{\rightleftharpoons}} V_{n+m} + DEG \tag{9h}$$

$$P_n + W_m \underset{2(n+m-1)k'_{pd}}{\overset{2k_{pd}}{\rightleftharpoons}} S_{n+m} + DEG \tag{9i}$$

$$Q_n + W_m \underset{2(n+m-1)k'_{pd}}{\overset{k_{pd}}{\rightleftharpoons}} U_{n+m} + DEG \tag{9j}$$

$$S_n + W_m \underset{4(n+m-1)k'_{pd}}{\overset{k_{pd}}{\rightleftharpoons}} Y_{n+m} + DEG \tag{9k}$$

$$T_n + W_m \underset{2(n+m-1)k'_{pd}}{\overset{k_{pd}}{\rightleftharpoons}} W_{n+m} + DEG \tag{9l}$$

$$P_n + Z_m \underset{2(n+m-1)k'_{pd}}{\overset{4k_{pd}}{\rightleftharpoons}} T_{n+m} + DEG \tag{9m}$$

$$Q_n + Z_m \underset{2(n+m-1)k'_{pd}}{\overset{k_{pd}}{\rightleftharpoons}} V_{n+m} + DEG \tag{9n}$$

$$S_n + Z_m \underset{2(n+m-1)k'_{pd}}{\overset{k_{pd}}{\rightleftharpoons}} W_{n+m} + DEG \tag{9o}$$

$$T_n + Z_m \underset{4(n+m-1)k'_{pd}}{\overset{k_{pd}}{\rightleftharpoons}} Z_{n+m} + DEG \tag{9p}$$

where k_{pd} is the forward rate constant for the reaction of the diethylene glycol end group with the hydroxyethyl end group and k'_{pd} the reverse rate constant

for the reaction of the hydroxyl group in DEG with the diester group in the polymer chain. Note that the factors (4 or 2) appear in front of the rate constants of reverse reactions due to the same reason as the reverse esterification reactions explained above.

It has been reported that the molecular weight of PET may reach a maximum value during the melt-polycondensation reaction and that the acid content of a polymer sample increases at elevated temperature.[15-17] This is due to the thermal degradation reactions in the polymer melt at high temperature. The rate of the degradation reaction depends largely on the reaction temperature as well as on the catalyst used in the transesterification and polycondensation stages. The mechanism of degradation reaction of diester groups is shown in Table III [reaction (i)]. In order to reduce the number of polymeric species to be included in our model, the activity of vinyl end group is assumed to be equal to that of the hydroxyethyl end group; therefore, no additional species have to be defined for the reactions involving the vinyl end group. Under this assumption, the molecular species having vinyl end groups are substituted with the corresponding species having hydroxyethyl end groups. Since the amount of vinyl end group produced is very small, the unbalance on the total mass caused by this substitution is negligible. This method was also used in Ref. 7. The molecular species model for the degradation of diester groups can be represented as follows (for $n \geq 2$, $1 \leq r \leq n-1$):

$$\mathrm{P}_n \xrightarrow{2(n-1)k_g} \mathrm{P}_{n-r} + \mathrm{S}_r \tag{10a}$$

$$\mathrm{Q}_n \xrightarrow{(n-1)k_g} \mathrm{P}_{n-r} + \mathrm{U}_r \tag{10b}$$

$$\mathrm{Q}_n \xrightarrow{(n-1)k_g} \mathrm{Q}_{n-r} + \mathrm{S}_r \tag{10c}$$

$$\mathrm{R}_n \xrightarrow{2(n-1)k_g} \mathrm{Q}_{n-r} + \mathrm{U}_r \tag{10d}$$

$$\mathrm{S}_n \xrightarrow{(n-1)k_g} \mathrm{S}_{n-r} + \mathrm{S}_r \tag{10e}$$

$$\mathrm{S}_n \xrightarrow{(n-1)k_g} \mathrm{P}_{n-r} + \mathrm{Y}_r \tag{10f}$$

$$\mathrm{T}_n \xrightarrow{(n-1)k_g} \mathrm{S}_{n-r} + \mathrm{T}_r \tag{10g}$$

$$\mathrm{T}_n \xrightarrow{(n-1)k_g} \mathrm{P}_{n-r} + \mathrm{W}_r \tag{10h}$$

$$\mathrm{U}_n \xrightarrow{(n-1)k_g} \mathrm{Q}_{n-r} + \mathrm{Y}_r \tag{10i}$$

$$\mathrm{U}_n \xrightarrow{(n-1)k_g} \mathrm{S}_{n-r} + \mathrm{U}_r \tag{10j}$$

$$\mathrm{V}_n \xrightarrow{(n-1)k_g} \mathrm{Q}_{n-r} + \mathrm{W}_r \tag{10k}$$

$$\mathrm{V}_n \xrightarrow{(n-1)k_g} \mathrm{U}_{n-r} + \mathrm{T}_r \tag{10l}$$

$$\mathrm{W}_n \xrightarrow{(n-1)k_g} \mathrm{S}_{n-r} + \mathrm{W}_r \tag{10m}$$

$$\mathrm{W}_n \xrightarrow{(n-1)k_g} \mathrm{T}_{n-r} + \mathrm{Y}_r \tag{10n}$$

$$\mathrm{Y}_n \xrightarrow{2(n-1)k_g} \mathrm{S}_{n-r} + \mathrm{Y}_r \tag{10o}$$

$$\mathrm{Z}_n \xrightarrow{2(n-1)k_g} \mathrm{T}_{n-r} + \mathrm{W}_r \tag{10p}$$

where k_g is the rate constant for the degraded reaction of the diester group in the polymer chain.

There are a number of interchange reactions occurring simultaneously in the PET polycondensation. These reactions do not change the concentration of each species nor the degree of polymerization, but they do change the molecular weight distribution of the final polymer. Three types of interchange reactions, namely intermolecular alcoholysis, intermolecular acidolysis, and transesterification, are possible for the species having hydroxyethyl end group or acid end group. To reduce the complexity of our model, only the alcoholysis reactions related with P species, the most abundant species in the reaction mixture, are considered [reaction (k) in Table III]:

$$P_n + P_m \underset{4(n+m-r-1)(r-1)k'_{rg}}{\overset{4(n-1)(m-1)k_{rg}}{\rightleftharpoons}} P_{n+m-r} + P_r \quad (n, m \geq 1, 1 \leq r \leq n+m-1) \quad (11a)$$

$$P_n + Q_m \underset{2(n+m-r-1)(r-1)k'_{rg}}{\overset{2(n-1)(m-1)k_{rg}}{\rightleftharpoons}} P_{n+m-r} + Q_r \quad (n, m \geq 1, 1 \leq r \leq n+m-1) \quad (11b)$$

$$P_n + S_m \underset{2(n+m-r-1)(r-1)k'_{rg}}{\overset{2(n-1)(m-1)k_{rg}}{\rightleftharpoons}} P_{n+m-r} + S_r \quad (n, m \geq 1, 1 \leq r \leq n+m-1) \quad (11c)$$

$$P_n + T_m \underset{2(n+m-r-1)(r-1)k'_{rg}}{\overset{2(n-1)(m-1)k_{rg}}{\rightleftharpoons}} P_{n+m-r} + T_r \quad (n, m \geq 1, 1 \leq r \leq n+m-1) \quad (11d)$$

where k_{rg} and k'_{rg} are the rate constants for the reactions of hydroxyethyl end group with the diester group in the polymer chain. The factors 4, $(n-1)$, and $(m-1)$, represent the total number of hydroxyethyl end groups and number of diester groups in the two reacting species, respectively.

GOVERNING EQUATIONS FOR A SEMIBATCH PREPOLYCONDENSATION REACTOR

According to the chemical reaction scheme discussed in the previous section, the prepolycondensation mixture will contain mainly 10 polymeric species and small amount of three volatile species (ethylene glycol, diethylene glycol, and water) and catalyst. Methanol and acetaldehyde will vaporize instantaneously upon formation, and it will be safe to assume that they are not trapped in the reaction mixture. Based on the ten major reactions between the functional groups as shown in Table II and the assumption of perfect mixing and constant melt density, one can derive a set of mass balances which constitute the mathematical model for this system under isothermal condition.

Since the reaction volume decreases with conversion due to the continuous removal of the condensation byproducts, it will be more convenient to use the material balance equations based on the number of moles of each species in the reactor. Assuming that the reactivities of various functional groups do not depend on the polymer chain length, we can develop the rate expressions for various reaction steps as follows.

For growing polymers ($n \geq 1$):

$$\frac{dP_n}{dt} = \frac{N}{V^2}\{2G(k_iQ_n + k_{eg}S_n) - P_n[2k_5 + (n-1)k_1 + 2(n-3)k_{rg}C_{P0} + 4k_{rg}\sum_{n=1}^{\infty} n(2P_n + Q_n + S_n + T_n) - 4k_{rg}\sum_{n=1}^{\infty}(n-1)P_n] + \sum_{r=1}^{n-1}[2P_r(k_tQ_{n-r} + k_pP_{n-r} + k_eS_{n-r} + k_{pd}T_{n-r})] + (k_2 + k_4)C_P + 2k_{rg}C_{P0}\sum_{m=n+1}^{\infty} P_m + 4k_{rg}\sum_{m=1}^{n-1}\sum_{l=n-m+1}^{\infty} P_m(P_l + Q_l + S_l + T_l)\} \quad (12)$$

$$\frac{dQ_n}{dt} = \frac{N}{V^2}\{2G(2k_iR_n + k_{eg}U_n) - Q_n[k_5 + 2k_iG + k_tC_{P0} + (n-1)k_1 + 2(2n-3)k_{rg}\sum_{n=1}^{\infty} P_n + 2k_{rg}\sum_{n=1}^{\infty} nP_n] + \sum_{r=1}^{n-1}[Q_n(k_tQ_{n-r} + 2k_pP_{n-r} + k_eS_{n-r} + k_{pd}T_{n-r}) + 2P_r(2k_tR_{n-r} + k_eU_{n-r} + k_{pd}V_{n-r})] + (k_2 + k_4)C_T + 4k_{rg}\sum_{n=1}^{\infty} P_n\sum_{m=n+1}^{\infty} Q_m + 2k_{rg}\sum_{m=1}^{n-1}\sum_{l=n-m+1}^{\infty} Q_mP_l\} \quad (13)$$

$$\frac{dR_n}{dt} = \frac{N}{V^2}\left\{-R_n[4k_iG + k_tC_{P0} + (n-1)k_1] + \sum_{r=1}^{n-1}\left[Q_r\left(2k_tR_{n-r} + \frac{1}{2}k_pQ_{n-r} + k_eU_{n-r} + k_{pd}V_{n-r}\right)\right]\right\} \quad (14)$$

$$\frac{dS_n}{dt} = \frac{N}{V^2}\{2G(k_iU_n + 2k_{eg}Y_n) + 2k_3P_n - S_n[k_5 + 2k_{eg}G + k_eC_{P0} + (n-1)k_1 + 2(2n-3)k_{rg}\sum_{n=1}^{\infty} P_n + 2k_{rg}\sum_{n=1}^{\infty} nP_n] + \sum_{r=1}^{n-1}[S_r(k_tQ_{n-r} + 2k_pP_{n-r} + k_eS_{n-r} + k_{pd}T_{n-r}) + 2P_r(k_tU_{n-r} + k_{pd}W_{n-r} + 2k_eY_{n-r})] + (k_2 + k_4)C_E + 4k_{rg}\sum_{n=1}^{\infty} P_n\sum_{m=n+1}^{\infty} Q_m + 2k_{rg}\sum_{m=1}^{n-1}\sum_{l=n-m+1}^{\infty} Q_mP_l\} \quad (15)$$

$$\frac{dT_n}{dt} = \frac{N}{V^2}\{2G(k_iU_n + k_{eg}W_n) + 2k_dP_nC_{P0} - T_n[k_5 + k_{pd}C_{P0} + (n-1)k_1 + 2(2n-3)k_{rg}\sum_{n=1}^{\infty} P_n + 2k_{rg}\sum_{n=1}^{\infty} nP_n] + \sum_{r=1}^{n-1}[T_r(k_tQ_{n-r} + 2k_pP_{n-r} + k_eS_{n-r} + k_{pd}T_{n-r}) + 2P_r(k_tV_{n-r} + k_eW_{n-r} + 2k_{pd}Z_{n-r})]$$

$$+ (k_2 + k_4) C_D + 2k'_{pd} DC_P + 4k_{rg} \sum_{n=1}^{\infty} P_n \sum_{m=n+1}^{\infty} T_m + 2k_{rg} \sum_{m=1}^{n-1} \sum_{l=n-m+1}^{\infty} T_m P_l \} \quad (16)$$

$$\frac{dU_n}{dt} = \frac{N}{V^2} \{ k_3 Q_n - U_n [2(k_i + k_{eg}) G + (k_t + k_e) C_{P0} + (n-1) k_1] + \sum_{r=1}^{n-1} [Q_r (k_t U_{n-r} + k_p S_{n-r} + k_{pd} W_{n-r} + 2k_e Y_{n-r}) + S_r (2k_t R_{n-r} + k_e U_{n-r} + k_{pd} V_{n-r})] + k_4 C_T \} \quad (17)$$

$$\frac{dV_n}{dt} = \frac{N}{V^2} \{ k_d Q_n C_{P0} - V_n [2k_i G + (k_t + k_{pd}) C_{P0} + (n-1) k_1] + \sum_{r=1}^{n-1} [Q_r (k_t V_{n-r} + k_p T_{n-r} + k_e W_{n-r} + 2k_{pd} Z_{n-r}) + T_r (2k_t R_{n-r} + k_e U_{n-r} + k_{pd} V_{n-r})] + 2k'_{pd} DC_T \} \quad (18)$$

$$\frac{dW_n}{dt} = \frac{N}{V^2} \{ k_d S_n C_{P0} + k_3 T_n - W_n [2k_{eg} G + (k_t + k_{pd}) C_{P0} + (n-1) k_1] + \sum_{r=1}^{n-1} [S_r (k_t V_{n-r} + k_p T_{n-r} + k_e W_{n-r} + 2k_{pd} Z_{n-r}) + T_r (k_t U_{n-r} + k_{pd} W_{n-r} + 2k_e Y_{n-r})] + k_4 C_D + 2k'_{pd} DC_E \} \quad (19)$$

$$\frac{dY_n}{dt} = \frac{N}{V^2} \left\{ k_3 S_n - Y_n [4k_{eg} G + 2k_e C_{P0} + (n-1) k_1] + \sum_{r=1}^{n-1} \left[S_r \left(k_t U_{n-r} + \frac{1}{2} k_p S_{n-r} + k_{pd} W_{n-r} + 2k_e Y_{n-r} \right) \right] + k_4 C_E \right\} \quad (20)$$

$$\frac{dZ_n}{dt} = \frac{N}{V^2} \left\{ k_d T_n C_{P0} - Z_n [2k_{pd} C_{P0} + (n-1) k_1] + \sum_{r=1}^{n-1} \left[T_r \left(k_t U_{n-r} + \frac{1}{2} k_p T_{n-r} + k_e W_{n-r} + 2k_{pd} Z_{n-r} \right) \right] + 2k'_{pd} C_D \right\} \quad (21)$$

For volatile species:

$$\frac{dM}{dt} = \frac{N}{V^2} (2k_i G + k_t C_{P0}) C_{T0} \quad (22)$$

$$\frac{dA}{dt} = \frac{N}{V^2} k_a C_{P0} \quad (23)$$

$$\frac{dG}{dt} = \frac{N}{V^2}\left\{\frac{1}{2}k_pC_{P0}^2 - k_p'G[\sum_{n=1}^{\infty} 2n(P_n + Q_n + R_n + S_n + T_n + U_n + V_n + W_n + Y_n + Z_n) - C_{P0} - C_{T0} - C_{E0} - C_{D0}] - 2k_{eg}GC_{E0} + k_{eg}'WC_{P0} - 2k_iGC_{T0} - 2k_tGC_{P0}\right\}, \quad G = \text{ethylene glycol} \quad (24)$$

$$\frac{dW}{dt} = \frac{N}{V^2}\{2k_{eg}GC_{E0} - k_{eg}'WC_{P0} + k_eC_{P0}C_{E0} - k_e'W[\sum_{n=1}^{\infty} 2n(P_n + Q_n + R_n + S_n + T_n + U_n + V_n + W_n + Y_n + Z_n) - C_{P0} - C_{T0} - C_{E0} - C_{D0}]\} \quad (25)$$

$$\frac{dD}{dt} = \frac{N}{V^2}\{2k_fGC_{P0} + k_{pd}C_{P0}C_{D0} - 2k_{pd}'D[\sum_{n=1}^{\infty} 2n(P_n + Q_n + R_n + S_n + T_n + U_n + V_n + W_n + Y_n + Z_n) - C_{P0} - C_{T0} - C_{E0} - C_{D0}]\}, \quad D = \text{diethylene glycol} \quad (26)$$

where upper case symbols represent the number of moles of each species, V the volume of reaction mixture, and N the initial number of moles of catalyst. The following variables combining some concentrations and rate constants are also defined and used in the modeling equations in order to simplify the rate expressions:

$$C_{P0} = \sum_{n=1}^{\infty}(2P_n + Q_n + S_n + T_n) \quad \text{(total hydroxyethyl groups)} \quad (27a)$$

$$C_{T0} = \sum_{n=1}^{\infty}(Q_n + 2R_n + U_n + V_n) \quad \text{(total methyl ester groups)} \quad (27b)$$

$$C_{E0} = \sum_{n=1}^{\infty}(S_n + U_n + W_n + 2Y_n) \quad \text{(total carboxyl acid groups)} \quad (27c)$$

$$C_{D0} = \sum_{n=1}^{\infty}(T_n + V_n + W_n + 2Z_n) \quad \text{(total DEG end groups)} \quad (27d)$$

$$C_P = \sum_{m=n+1}^{\infty}(2P_m + Q_m + S_m + T_m) \quad \text{(hydroxyethyl groups)} \quad (27e)$$

$$C_T = \sum_{m=n+1}^{\infty}(Q_m + 2R_m + U_m + V_m) \quad \text{(methyl ester groups)} \quad (27f)$$

$$C_E = \sum_{m=n+1}^{\infty}(S_m + U_m + W_m + 2Y_m) \quad \text{(carboxyl acid groups)} \quad (27g)$$

$$C_D = \sum_{m=n+1}^{\infty}(T_m + V_m + W_m + 2Z_m) \quad \text{(DEG end groups)} \quad (27h)$$

$$k_1 = 2k'_pG + 2k'_eW + 4k'_{pd}D + 2k'_g \tag{27i}$$

$$k_2 = 2k'_pG + 2k'_{pd}D \tag{27j}$$

$$k_3 = k_a + 2k_fG + k_dC_{P0} + k'_{eg}W \tag{27k}$$

$$k_4 = k'_eW + k_g \tag{27l}$$

$$k_5 = k_tC_{T0} + (k_p + 2k_d)C_{P0} + k_eC_{E0} + k_{pd}C_{D0} + k_a + 2k_fG + k'_{eg}W \tag{27m}$$

In order to compute the molecular weight averages of polymers, the molecular weight moments are defined as follows:

$$\lambda_{\xi,k} \equiv \sum_{n=1}^{\infty} n^k \xi_n \qquad (\xi = P, Q, R, S, T, U, V, W, Y, Z) \tag{28}$$

where $\lambda_{\xi,k}$ denotes the kth moment of polymeric species ξ. The overall number average chain length (X_N) and the weight average chain length (X_W) are defined by

$$X_N = \frac{\sum_{\xi} \lambda_{\xi,1}}{\sum_{\xi} \lambda_{\xi,0}} \qquad (\xi = P, Q, R, S, T, U, V, W, Y, Z) \tag{29a}$$

$$X_W = \frac{\sum_{\xi} \lambda_{\xi,2}}{\sum_{\xi} \lambda_{\xi,1}} \qquad (\xi = P, Q, R, S, T, U, V, W, Y, Z) \tag{29b}$$

The polydispersity is a measure of molecular weight distribution broadening and is defined by

$$\text{PD} = X_W/X_N \tag{29c}$$

Using the rate expressions for various species and the moments defined above, one can derive the molecular weight moment equations and they are given in the Appendix.

For the calculation of the concentrations of volatile species in the reaction mass and in the vapor phase, a quasisteady state assumption is used for the vapor–liquid equilibrium in small increments of time.[18] The vapor phase is assumed to follow the ideal gas law

$$p_i = py_i \tag{30}$$

where p is the total pressure and p_i and y_i are the partial pressure and mole fraction of species i, respectively. In the liquid phase, either Raoult's law or the Flory–Huggins model can be used. Under vapor–liquid equilibrium, the partial pressure of the volatile species in the liquid phase can be generally represented as

$$p_i = \gamma_i p_i^{\text{sat}} x_i \tag{31}$$

where γ_i, p_i^{sat}, and x_i are the activity coefficient, saturated vapor pressure, and mole fraction of component i, respectively. $\gamma_i = 1$ for Raoult's law and the Flory–Huggins model γ is given by[19]

$$\ln \gamma_1 = \ln[1 - (1 - 1/m)\Phi_2] + (1 - 1/m)\Phi_2 + \chi\Phi_2^2 \tag{32}$$

where component 1 and 2 represent the solvent and the solute, Φ_i the volume fraction of component i, χ the polymer interaction parameter, and m the ratio of molar volumes of solute and solvent. In our polymer melt system, the polymer is the solute and the volatile species the solvent. Since the mole fraction of volatile species is very small under high reaction temperature and vacuum condition, $\Phi_2 \rightarrow 1$, and thus the Flory–Huggins equation is reduced to

$$\gamma_1 = (1/m) \exp(1 - 1/m + \chi) \tag{33}$$

Mass balance equations and the vapor–liquid equilibrium equation are combined and solved simultaneously to calculate the concentrations of volatile species in the liquid phase and the vapor phase. The volume of the reaction mixture (melt phase) is updated by subtracting the equivalent volume of condensate removed from the reactor. The kth moment equations, as shown in the Appendix, contain $(k + 1)$th moment terms, showing the coupled nature of these equations when the reverse reactions are involved. The values of the third moment for each species are estimated by using the moment closing formula,[20]

$$\lambda_{\xi,3} = \frac{\lambda_{\xi,2}(2\lambda_{\xi,2}\lambda_{\xi,0} - \lambda_{\xi,1}^2)}{\lambda_{\xi,1}\lambda_{\xi,0}} \tag{34}$$

Due to the scarcity of experimental data on many of the reactions considered in our model, the rate constants used by Ravindranath and Mashelkar[4] for their simulations are also used in our model simulations. The numerical values of the parameters and physical constants used in the present work are shown in Table IV. Note that, since catalyst concentration is considered separately, the rate constants given by Ravindranath and Mashelkar have been divided by the initial catalyst concentration to obtain the intrinsic rate constants. In addition to those parameters listed in Table IV, four reactor operating variables, e.g., initial composition, reaction temperature, pressure, and catalyst concentration, must also be specified. The base operating conditions chosen in our model simulations are:

Initial composition: 61% [BHET], 38% [MHET], and 1% [DMT]
(80% conversion of methyl ester group)
Temperature: 280°C
Pressure: 20 torr
Catalyst concentration: 0.05 wt % Sb_2O_3

Considering the fact that the conversion of methyl ester groups or DMT is in the range of 70–90% under practical process conditions of melt transesterification, we have chosen a 61/38/1 mixture of BHET, MHET, and DMT as a

TABLE IV
Numerical Values of Physical Constants and Parameters

k_p	$7.9286 \times 10^8 \exp(-18500/RT)$	L^2/mol^2 min
k'_p	$3.1714 \times 10^9 \exp(-18500/RT)$	L^2/mol^2 min
k_t	$2.3320 \times 10^7 \exp(-15000/RT)$	L^2/mol^2 min
k_i	$4.6640 \times 10^7 \exp(-15000/RT)$	L^2/mol^2 min
k_a	$4.8505 \times 10^{10} \exp(-29800/RT)$	L^2/mol^2 min
k_{eg}	$1.2126 \times 10^9 \exp(-17600/RT)$	L^2/mol^2 min
k'_{eg}	$4.8504 \times 10^8 \exp(-17600/RT)$	L^2/mol^2 min
k_e	$1.2126 \times 10^9 \exp(-17600/RT)$	L^2/mol^2 min
k'_e	$9.7008 \times 10^8 \exp(-17600/RT)$	L^2/mol^2 min
k_f	$4.8505 \times 10^{10} \exp(-29800/RT)$	L^2/mol^2 min
k_d	$4.8505 \times 10^{10} \exp(-29800/RT)$	L^2/mol^2 min
k_{pd}	$7.9286 \times 10^8 \exp(-18500/RT)$	L^2/mol^2 min
k'_{pd}	$1.5857 \times 10^9 \exp(-18500/RT)$	L^2/mol^2 min
k_g	$4.1975 \times 10^{12} \exp(-37800/RT)$	L/mol min
k_{rg}	$7.9286 \times 10^8 \exp(-18500/RT)$	L^2/mol^2 min
p_{EG}^{sat}	$10^{(21.61-3729/T-4.042 \log_{10} T)}$	mm Hg
p_W^{sat}	$10^{(8.6041-1757.853/(T-33.274))}$	mm Hg
p_{DEG}^{sat}	$\exp[17.0326 - 4122.52/T - 122.5)]$	mm Hg
V_0	0.3	L
ρ	1.0	kg/L
χ	0.5	

base case for the initial prepolymer composition. It is also assumed that oligomerization is not significant in the first stage.

RESULTS AND DISCUSSION

Polymer Molecular Weight

The molecular weight (MW) of PET is one of the most important property parameters. In the prepolymerization stage, BHET and low molecular weight oligomers are transformed to polymers of relatively low molecular weight. Figures 2 shows the profiles of MW in a semibatch prepolymerization reactor under various reactor operating conditions (temperature, pressure, and content of methyl ester groups). Here X_{ME} denotes the fractional conversion of methyl ester groups at the end of the transesterification stage. Since, in general, the complete conversion of methyl ester groups is not achieved in the transesterification stage, these unreacted methyl ester groups are present at the beginning of the prepolymerization stage. Therefore $(1 - X_{ME})$ represents the relative amount of methyl ester groups in the reactor. First, note that under standard reactor operating conditions (e.g., 20 torr, 280°C), the number average chain length (NACL) is about 32 after 120 min. This is in quite good agreement with industrial practice.[1] As the reaction temperature is increased, the NACL also increases; however, at 300°C, the NACL profile approaches the apparent plateau after about 80 min and then slightly decreases afterward. This is due to the degradation reaction which becomes significant at high temperature. The similar behavior was observed experimentally by Tomita[16] and Yokoyama et al.[17] The

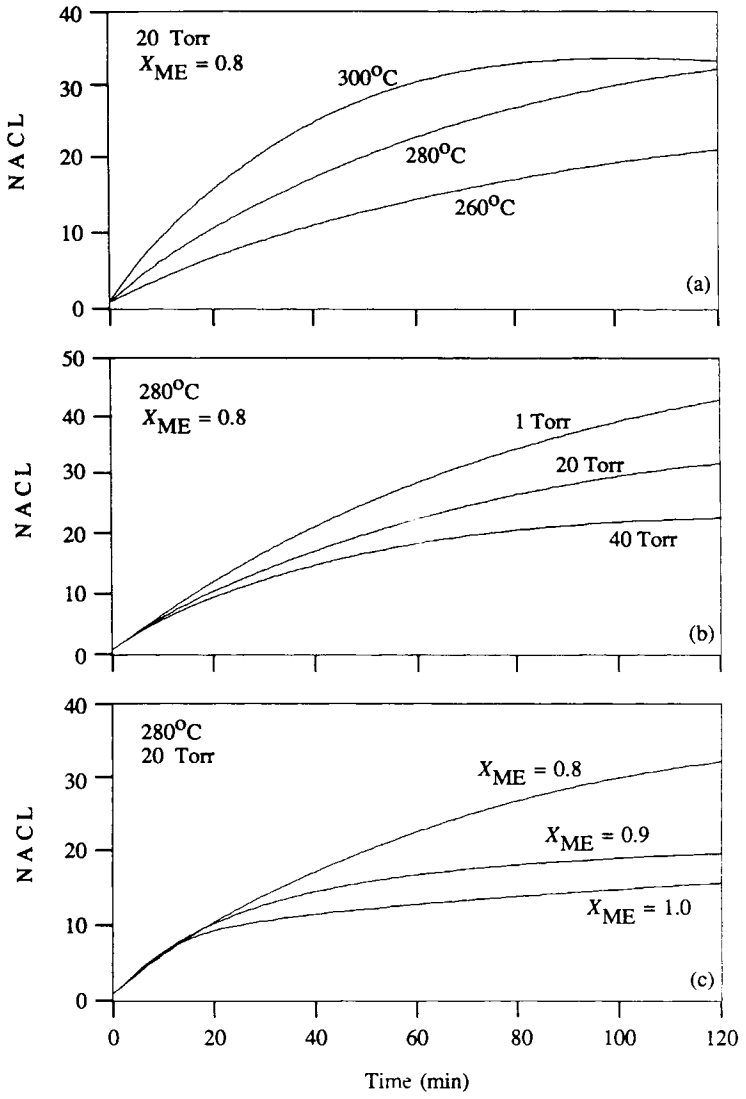

Fig. 2. Effects of temperature, pressure, and initial composition on the number average chain length of polymer.

NACL profiles shown in Figure 2 are quite different from Ref. 4 in which a functional group model was used: NACL increases continuously without showing a sign of level-off (e.g., 280°C, 20 mm Hg) after 1 h. With both reaction pressure and reaction time fixed at 20 torr and 120 min, the NACLs of PET have been computed and shown in Figure 3(a) as a function of initial methyl ester group concentration in the prepolymerization stage for various values of reactor temperature ranging from 260 to 300°C. It is interesting to observe that there exists an optimal initial methyl ester group concentration which gives the highest NACL of the polymer for a given reactor temperature. Figure 3(a) also shows the effect of degradation reaction: The highest NACL value is obtained at 280–290°C. The degradation reaction at high temperature is less pronounced when

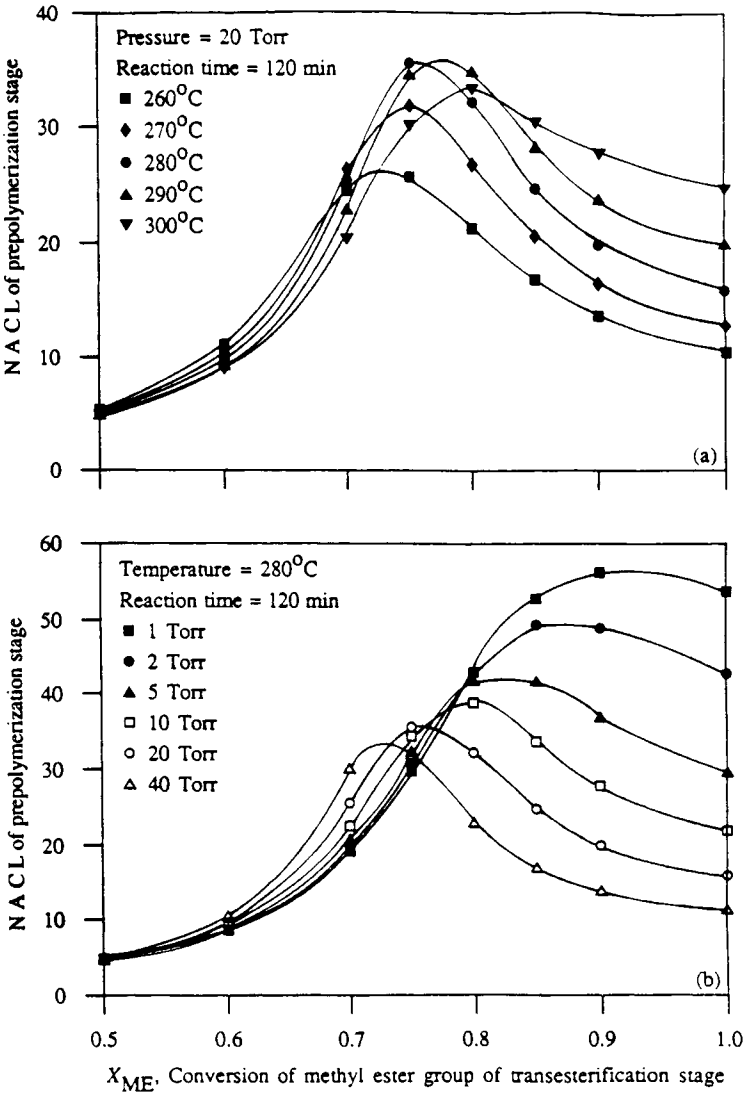

Fig. 3. Effect of methyl ester groups on the number average chain length of prepolymerization stage.

the initial methyl ester group concentration is low, i.e., high conversion of methyl ester group in the transesterification stage.

The effect of pressure on NACL is predictable as illustrated in Figure 2(b). As the reactor pressure is reduced, the higher molecular weight is obtained. Note, however, that, at 280°C, the reduction in the reactor pressure from 20 to 1 torr results in only a slight increase in molecular weight and this is somewhat surprising. Figure 3(b), with both temperature and reaction time fixed instead of pressure as in Figure 3(a), shows why this phenomenon occurs. There also exists an optimal methyl ester group concentration which gives the highest NACL of the polymer for a given reactor pressure. However, as the pressure is reduced, the peak NACL value increases and the location of the peak is shifted

toward the right. At high pressure (e.g., 40 torr), the highest NACL is obtainable when one starts the prepolymerization after about 75% conversion of methyl ester groups is achieved in the transesterification stage. As less methyl ester groups are present at the beginning of the prepolymerization, the resulting NACL becomes lower. However, when very low pressure (e.g., 1 torr) is used, the NACL increases as less methyl ester groups are present at the beginning of the prepolymerization. Since it is practically quite difficult to maintain the reactor pressure at about 1 torr in stirred prepolymerization reactors, many industrial prepolymerization reactors are operated at about 10–40 torr. The result shown in Figure 3(b) suggests that the incomplete conversion of methyl ester groups in the transesterification stage may be beneficial in increasing the polymer molecular weight without employing very low pressure.

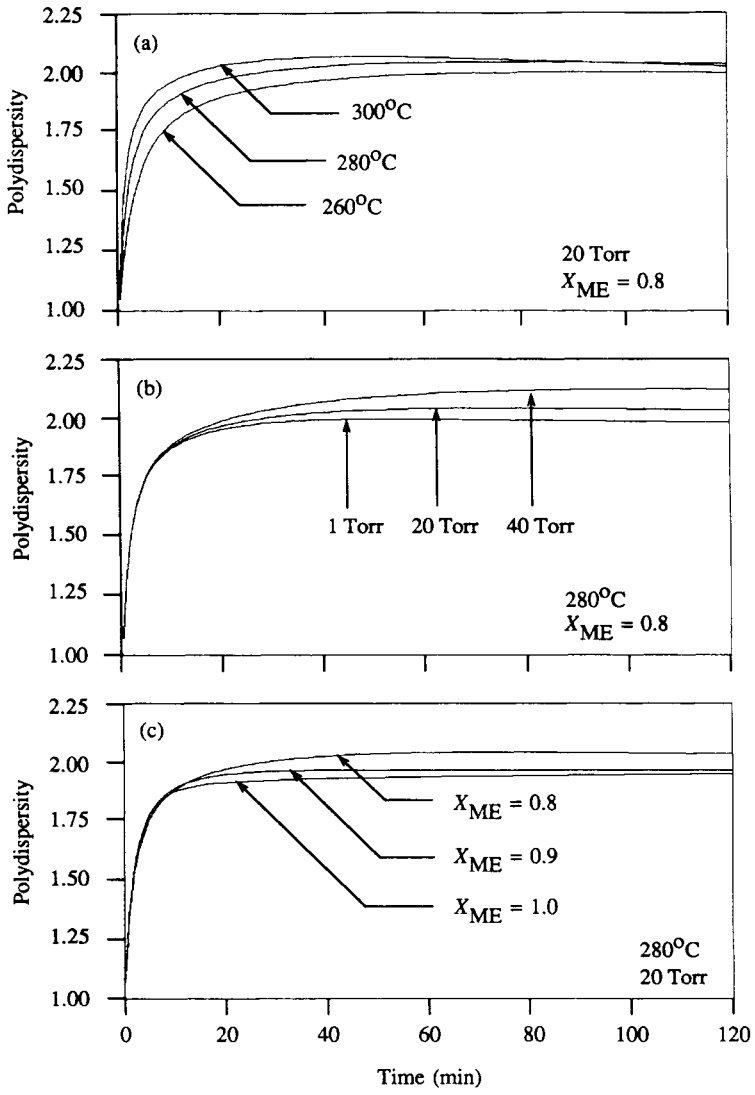

Fig. 4. Effects of temperature, pressure and initial composition on the polydispersity of polymer.

Figure 2(c) illustrates how NACL increases with time for different values of initial methyl ester group concentration. The high molecular weight observed when X_{ME} is high at low pressure is due to the fact that some methyl ester groups, by reacting with ethylene glycol, are converted to hydroxyethyl groups which are used in the polycondensation. Some methyl ester groups, by reacting with hydroxyethyl groups, also form polymer linkage directly via esterification (see Fig. 1). Ravindranath and Mashelkar[5] examined the effect of DMT addition on the molecular weight of the PET polymer under time-varying temperature and pressure conditions. Their results showed that the effect of DMT addition was detectable after about 1 h of reaction and the effect was not significant. Ault and Mellichamp[21] reported that the presence of methyl ester groups can decrease the NACL if the transesterification rate constant (k_t) is less than the polycondensation rate constant (k_p). Although the k_t value used in our simulation is smaller than k_p ($k_t/k_p = 0.711$, 280°C), the ester interchange rate constant (k_i) is much larger than k_p. In the presence of methyl ester groups, some EG formed in the polycondensation reaction are consumed by the ester interchange reaction and as a result the reverse reaction of polycondensation is suppressed. This implies that the increase in MW with more MHET in the reaction melt observed in Figure 2(c) is mostly due to the low concentration of ethylene glycol as shown later in Figure 5(c).

Figure 4 shows the polydispersity profiles at different reaction conditions. As expected, the polydispersity approaches 2.0 as the conversion increases but the polydispersity becomes slightly larger than 2 when the reactor is operated at high temperature, or high pressure (e.g., 40 torr), or in the presence of large amount of methyl ester group.

Ethylene Glycol

Ethylene glycol is the major condensation product in the polymerization stage and the rate of reverse reaction depends on the concentration of EG in the melt. Since vapor–liquid equilibrium is assumed throughout the reaction, the concentration profiles of ethylene glycol vary with the partial pressure and the operating pressure of the reactor as shown in Figure 5. It was shown in Figure 2(a) that the degradation reaction occurs at 300°C, leading to lower final MW. However, the concentration of ethylene glycol at 300°C is only slightly lower than that at 280°C after 120 min.

Hydroxyethyl End Groups

Figure 6 shows the concentration profiles of hydroxyethyl end groups under various conditions. Note that the conversion of hydroxyethyl group is a strong function of temperature. For example, the reaction time required to obtain high conversion of the end group (e.g., above 85%) increases significantly as the lower reaction temperature is used. As shown in Figures 2 and 3, the presence of methyl ester end groups tends to increase the polymer molecular weight for some cases by enhancing the conversion of hydroxyethyl groups. Note that although the difference in the final conversion of hydroxyethyl end groups at

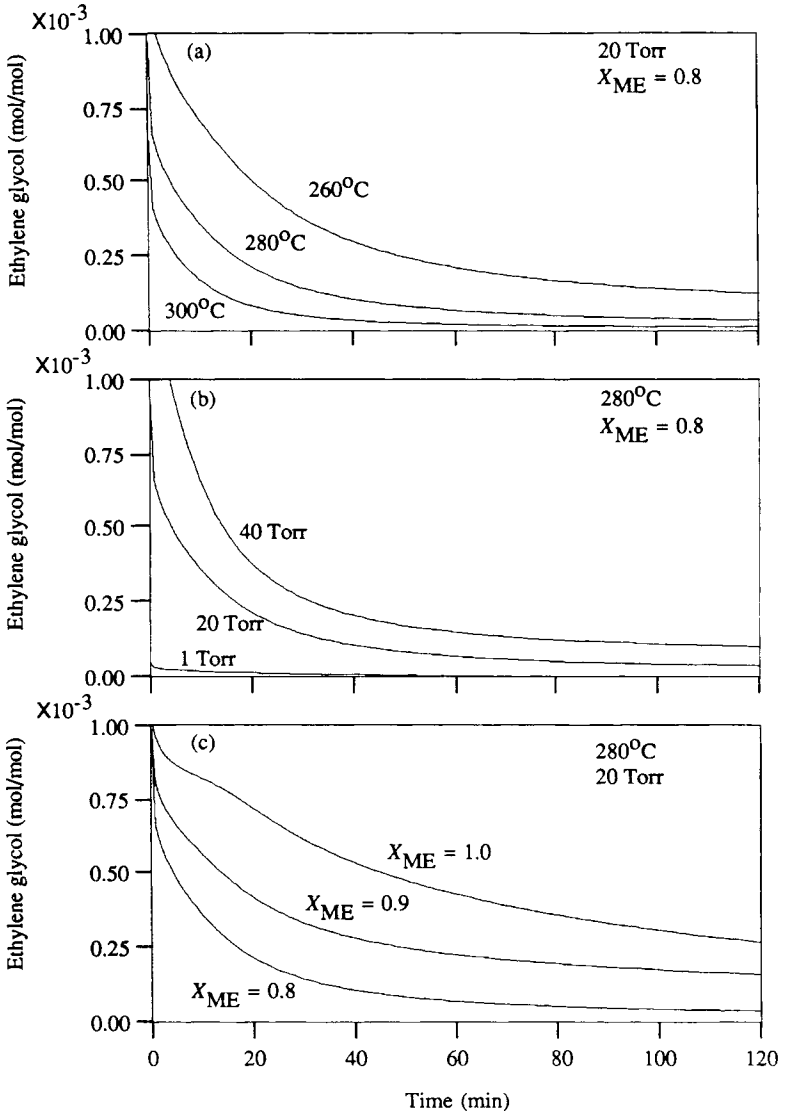

Fig. 5. Effects of temperature, pressure and initial composition on the concentration of ethylene glycol in the reaction mixture.

different operating conditions seems to be small, the resulting polymer molecular weights can be significantly different (cf. Fig. 2).

Carboxyl Acid Groups Formation

There are some contradictory reports on the formation of carboxyl acid end group in PET polymerization. In Ref. 4, it is shown that the acid end group concentration increases rapidly during the early reaction period and then decreases gradually as the polymerization proceeds. However, in Ref. 7, the acid

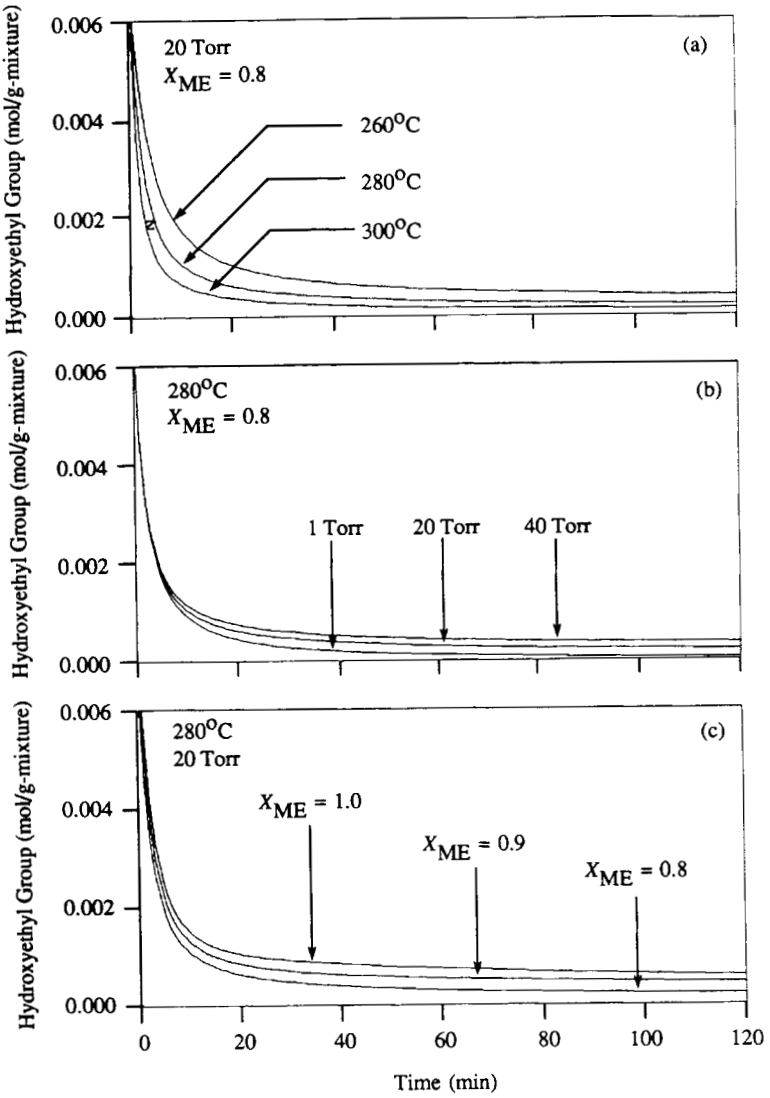

Fig. 6. Effects of temperature, pressure and initial composition on the concentration of hydroxyethyl end groups in the reaction mixture.

end group concentration is reported to increase almost linearly with time. Our simulation result, shown in Figure 7, indicates that the acid end group concentration increases continuously with reaction time and this is also in qualitative agreement with experimental data reported by Yokoyama et al.[22] and Yoda,[13] who also reports that any catalyst which facilitates the DEG formation reaction also promotes the carboxyl acid end group formation reaction. Note that the acid end group formation is little affected by the presence of methyl ester group in the initial reaction mixture but rather strongly influenced by reaction temperature and pressure. The acid groups concentration increases as the reaction temperature is increased and the pressure is reduced. Similar qualitative behavior was also reported in the experimental work by Yokoyama et al.[22]

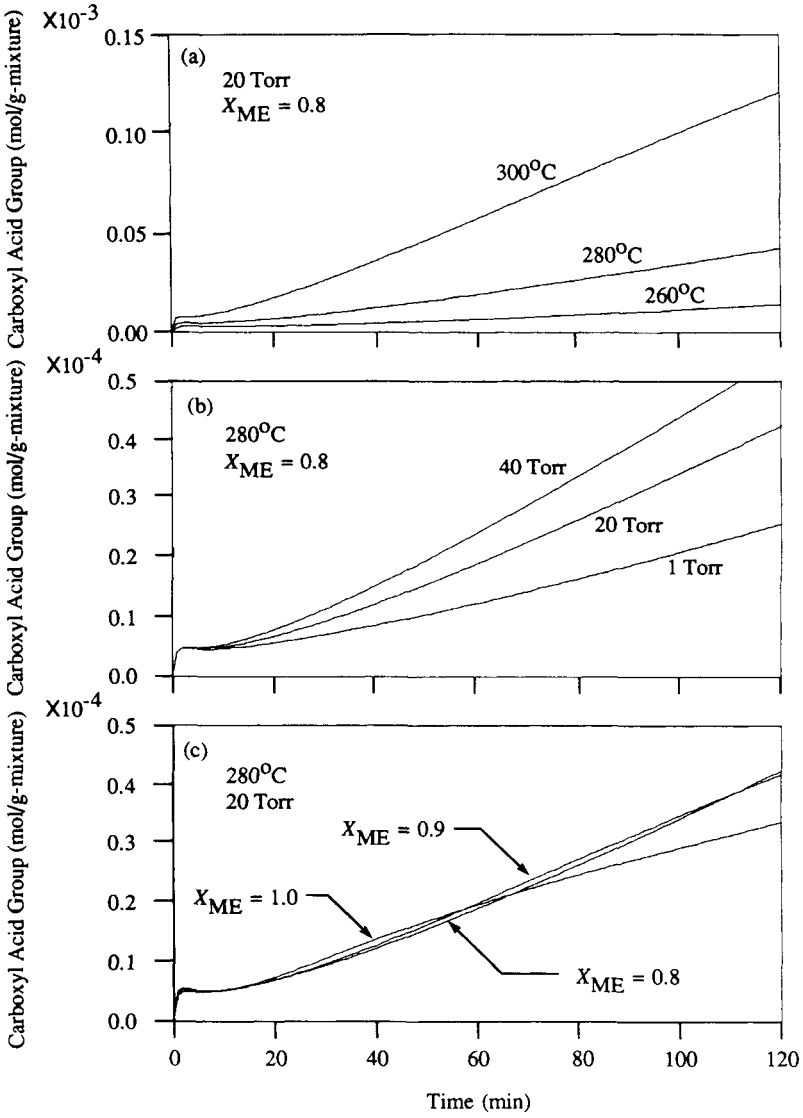

Fig. 7. Effects of temperature, pressure and initial composition of the concentration of carboxyl acid end groups in the reaction mixture.

Diethylene Glycol Formation

The presence of DEG in PET affects the crystalline content of polymers and results in reduced strength of oriented films and fibers. Figure 8 illustrates the weight fractions of free DEG and total DEG (free and incorporated) in the polymerizing mass for different reaction conditions. The predicted DEG weight fraction is somewhat lower than the reported value ($\sim$ 1 wt %).[23] Initially DEG concentration increases very rapidly due to the high concentration of hydroxyethyl groups in the reactor and then increases rather slowly. Note that the amount of free DEG is quite negligible. It is also interesting to observe that

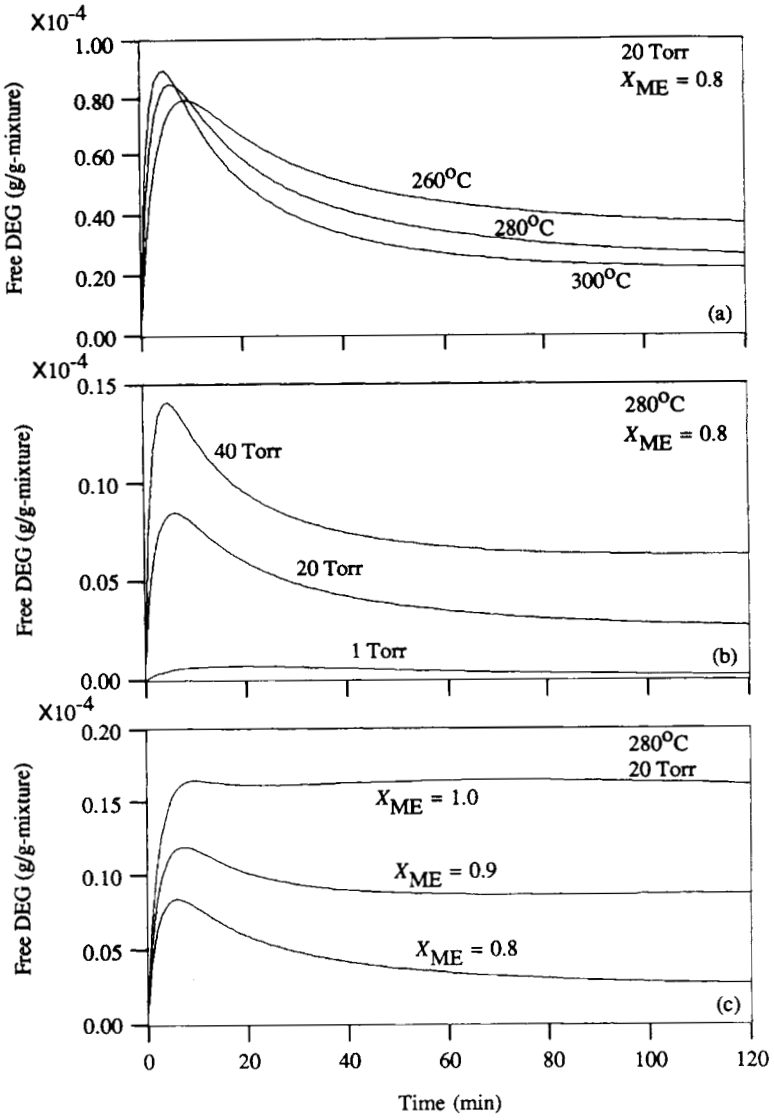

Fig. 8. Effects of temperature, pressure, and initial composition on the concentration of DEG in the reaction mixture.

when very high vacuum is applied (e.g., 1 torr), total DEG content decreases as the polymerization proceeds. This is because the intensive removal of free DEG occurs, enhancing the polycondensation reaction of DEG end groups which transfer one DEG end group to a ester linkage in polymer chain.

Acetaldehyde

As shown in Table III, acetaldehyde is formed by the degradation of hydroxyethyl end group to carboxyl acid end group. In the manufacture of PET (especially bottle grade), the control of acetaldehyde concentration is of prime importance because retained acetaldehyde can migrate to the beverage and

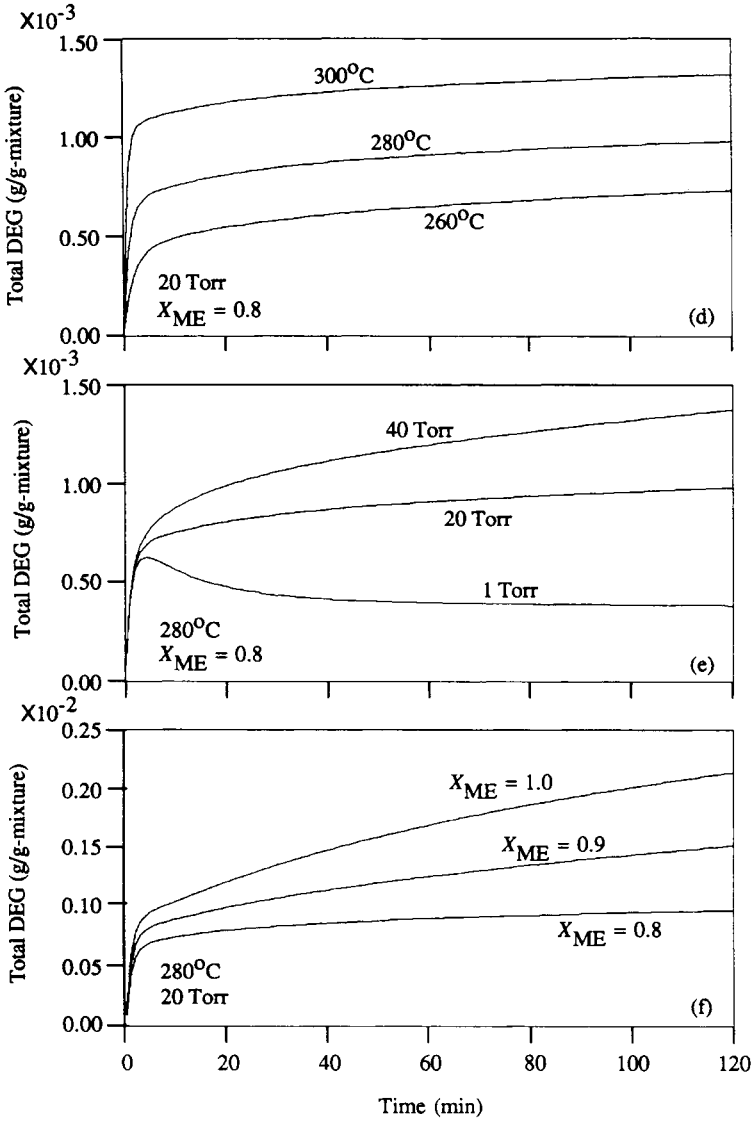

Fig. 8 *(Continued from the previous page)*

cause changes in taste.[24] Generation of acetaldehyde also occurs during the blow molding of PET bottles from PET resins.[25] It was also suggested that the discoloration of PET is due to polyenaldehydes resulting from the polymerization of acetaldehyde.[26] Although Figure 9 shows the weight fraction of acetaldehyde in the condensate, it shows qualitatively how much the formation of this byproduct is affected by the operating conditions. This information will be helpful in designing the finishing polymerization reactor where the mass transfer of volatile species should be considered. Figure 9 shows that acetaldehyde formation increases as the pressure increases and the temperature increases. Ravindranath and Mashelkar[4] reported similar behavior. The presence of methyl ester groups lowers the formation of acetaldehyde because the methyl

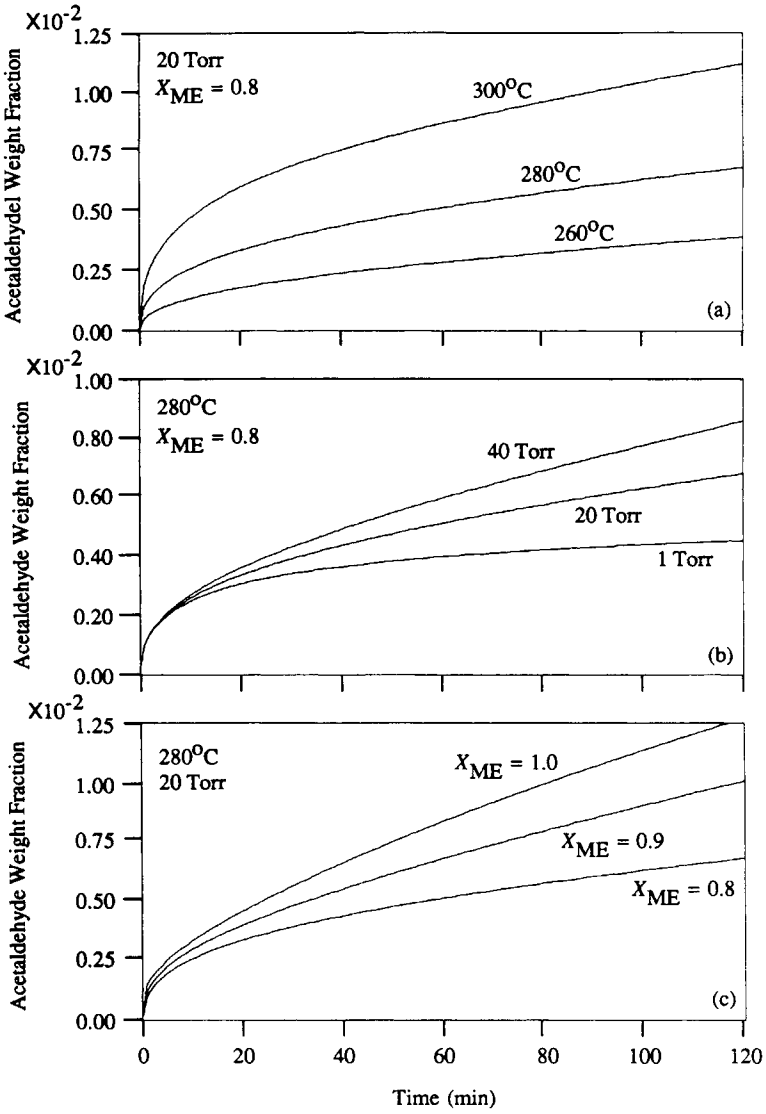

Fig. 9. Effects of temperature, pressure, and initial composition on the weight fraction of acetaldehyde in the condensate.

ester group reacts with hydroxyethyl end groups to form the polymer linkage and as a result less hydroxyethyl end groups become available for the degradation reaction.

Water Formation

A small amount of water is formed by esterification reactions [(g) and (h)]. Figure 10 shows that higher temperature and lower pressure give rise to reduced water concentration in the polymerizing mass. At typical prepolymerization condition (e.g., 280°C, 20 torr), water content is about 20 ppm. It is expected that the concentration of water will be further reduced in the finishing poly-

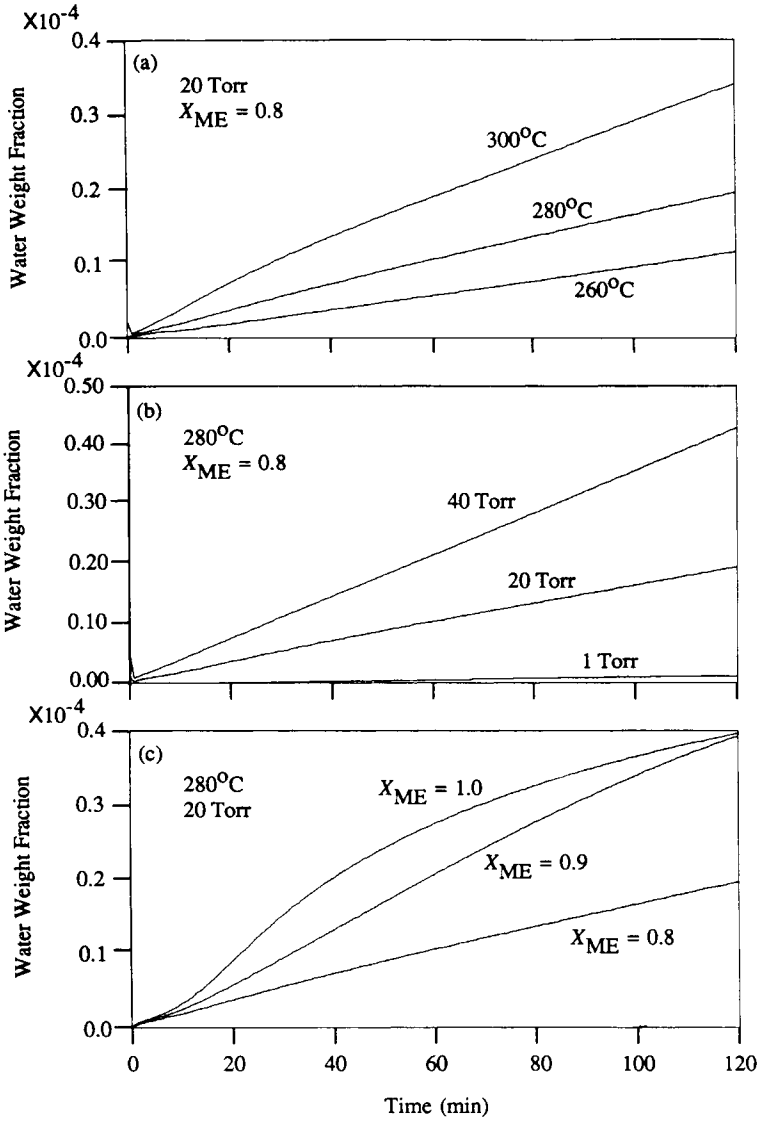

Fig. 10. Effects of temperature, pressure, and initial composition on the weight fraction of water in the reaction mixture.

merization stage in which very high vacuum (< 1.0 torr) and high temperature (~ 300°C) are employed. The presence of methyl ester groups slightly lower the water formation.

Composition and Molecular Weights of Polymeric Species

Figure 11 shows the mole fraction profiles of various polymeric species present in the reaction mixture for the two different initial compositions. Having hydroxyethyl groups on both ends and accounting for 80% of the initial reaction mixture after the end of the transesterification stage, species P is the most abundant species in the prepolymerization stage (about 70% throughout the

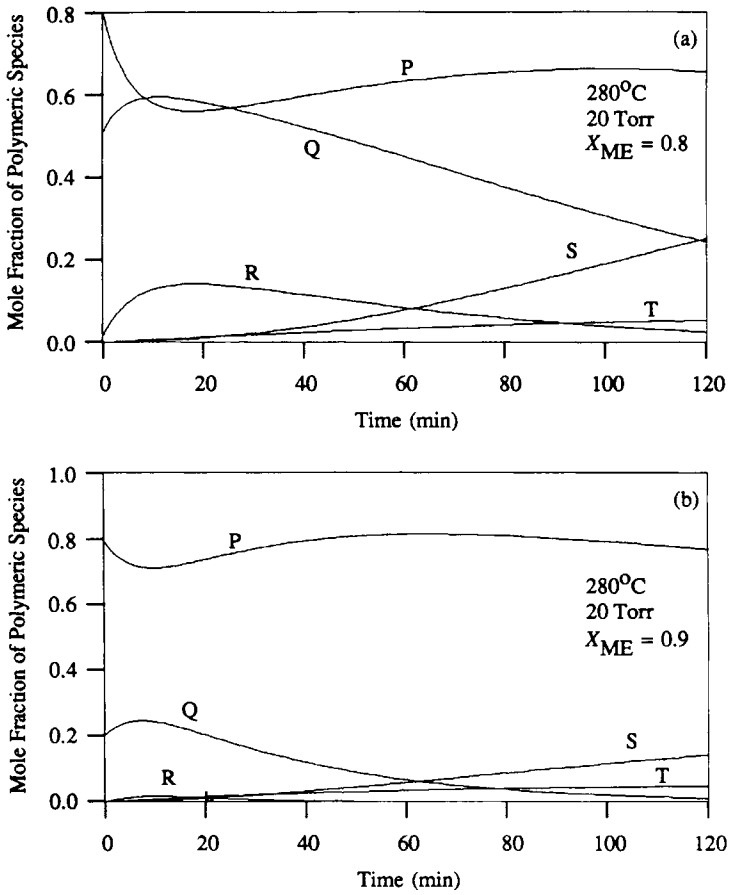

Fig. 11. Effect of initial composition on the mole fraction profiles of polymeric species.

reactions) as shown in Figure 11(b). Also note that, in Figure 11(a), there are considerable amounts of carboxyl acid end groups (S) produced and methyl ester groups (Q) left will be transferred to the finishing polymerization stage. Since these species are always shorter than species P, their existence will lower the overall molecular weight. The results shown in Figure 11 also explain why the MW is higher when less methyl ester group is present at low reaction pressure (e.g., 1 torr). Having one or two methyl ester group attached to the ends, both the species Q and R show a maximum concentration level in their profiles as they are the intermediates.

The number average chain length profiles of each polymeric species are shown in Figure 12. Note that the molecular weight of species Y containing carboxyl acid groups is the second highest of all species. However, the molecular weight of species R containing methyl ester groups is the lowest of all.

CONCLUDING REMARKS

In this work, we have developed a detailed molecular species model to describe the progress of prepolymerization of PET in a semibatch reactor. With Flory–

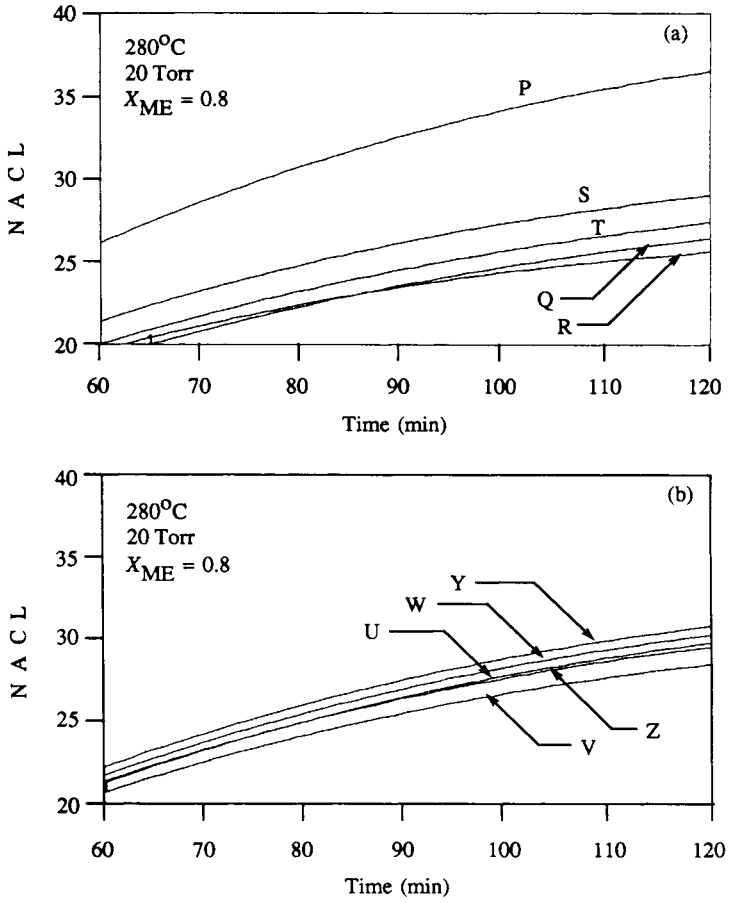

Fig. 12. Number average chain length profiles of polymeric species at base operating conditions.

Huggins vapor–liquid equilibrium model and realistic kinetic parameters incorporated, the model has been used to predict how the polymer chain growth occurs and how the concentrations of various side products and functional end groups vary under various reaction conditions. The initial conditions for the prepolymerization were chosen in such a way that incomplete conversion of methyl ester groups in the transesterification stage can be reflected in evaluating the behavior of semibatch prepolymerization. It has been observed that incomplete conversion of methyl ester groups in the transesterification stage may be beneficial in obtaining high molecular weight in the prepolymerization stage even when only moderate vacuum is applied. It has also been shown that the polydispersity value greater than 2.0 can be produced in the presence of methyl ester groups, at high reaction temperature, or at relatively high polymerization pressure (e.g., 40 torr). With the model presented in this work, it is possible to obtain deeper insight into the complex reaction kinetics in the PET prepolymerization stage.

This research was supported by the National Science Foundation and in part by the Systems Research Center at the University of Maryland.

APPENDIX: MOLECULAR WEIGHT MOMENT EQUATIONS

Polymeric species P_n:

$$\frac{d\lambda_{P,0}}{dt} = \frac{N}{V^2}\{2G(k_i\lambda_{Q,0} + k_{eg}\lambda_{S,0}) - 2k_5\lambda_{P,0} - k_1(\lambda_{P,1} - \lambda_{P,0}) + 2(C_{10} - k_p\lambda_{P,0})\lambda_{P,0} + (k_2 + k_4)(C_{P1} - C_{P0})\}$$

$$\frac{d\lambda_{P,1}}{dt} = \frac{N}{V^2}\{2G(k_i\lambda_{Q,1} + k_{eg}\lambda_{S,1}) - 2k_5\lambda_{P,1} - [k_1 + k_{rg}(C_{P0} + 2\lambda_{P,0})](\lambda_{P,2} - \lambda_{P,1}) + 2(C_{11} - k_p\lambda_{P,1})\lambda_{P,0} + 2(C_{10} - k_p\lambda_{P,0})\lambda_{P,1} + [\tfrac{1}{2}(k_2 + k_4) + 2k_{rg}\lambda_{P,0}](C_{P2} - C_{P1})\}$$

$$\frac{d\lambda_{P,2}}{dt} = \frac{N}{V^2}\{2G(k_i\lambda_{Q,2} + k_{eg}\lambda_{S,2}) - 2k_5\lambda_{P,2} - [k_1 + 2k_{rg}C_{P0}](\lambda_{P,3} - \lambda_{P,2}) + 2(C_{12} - k_p\lambda_{P,2})\lambda_{P,0} + 4(C_{11} - k_p\lambda_{P,1})\lambda_{P,1} + 2(C_{10} - k_p\lambda_{P,0})\lambda_{P,2} + [\tfrac{1}{6}(k_2 + k_4) + \tfrac{2}{3}k_{rg}\lambda_{P,0}](2C_{P3} - 3C_{P2} + C_{P1}) + (\tfrac{1}{3}k_{rg}C_{P0} - \tfrac{2}{3}k_{rg}\lambda_{P,0})(2\lambda_{P,3} - 3\lambda_{P,2} + \lambda_{P,1}) + 4k_{rg}\lambda_{P,1}(C_{P2} - C_{P1} + \lambda_{P,2} - \lambda_{P,1})\}$$

Polymeric species Q_n:

$$\frac{d\lambda_{Q,0}}{dt} = \frac{N}{V^2}\{2G(2k_i\lambda_{R,0} + k_{eg}\lambda_{U,0}) - (k_5 + 2k_iG + k_tC_{P0})\lambda_{Q,0} - k_1(\lambda_{Q,1} - \lambda_{Q,0}) + C_{10}\lambda_{Q,0} + 2C_{40}\lambda_{P,0} + (k_2 + k_4)(C_{T1} - C_{T0})\}$$

$$\frac{d\lambda_{Q,1}}{dt} = \frac{N}{V^2}\{2G(2k_i\lambda_{R,1} + k_{eg}\lambda_{U,1}) - (k_5 + 2k_iG + k_tC_{P0})\lambda_{Q,1} - (k_1 + 2k_{rg}\lambda_{P,0})(\lambda_{Q,2} - \lambda_{Q,1}) + C_{11}\lambda_{Q,0} + C_{10}\lambda_{Q,1} + 2C_{41}\lambda_{P,0} + 2C_{40}\lambda_{P,1} + \tfrac{1}{2}(k_2 + k_4)(C_{T2} - C_{T1}) + k_{rg}(\lambda_{P,2} - \lambda_{P,1})\lambda_{Q,0}\}$$

$$\frac{d\lambda_{Q,2}}{dt} = \frac{N}{V^2}\{2G(2k_i\lambda_{R,2} + k_{eg}\lambda_{U,2}) - (k_5 + 2k_iG + k_tC_{P0})\lambda_{Q,2} - (k_1 + 4k_{rg}\lambda_{P,0})(\lambda_{Q,3} - \lambda_{Q,2}) + C_{12}\lambda_{Q,0} + 2C_{11}\lambda_{Q,1} + C_{10}\lambda_{Q,2} + 2C_{42}\lambda_{P,0} + 4C_{41}\lambda_{P,1} + 2C_{40}\lambda_{P,2} + \tfrac{1}{6}(k_2 + k_4)(2C_{T3} - 3C_{T2} + C_{T1}) + \tfrac{2}{3}k_{rg}(2\lambda_{Q,3} - 3\lambda_{Q,2} + \lambda_{Q,1})\lambda_{P,0} + \tfrac{1}{3}k_{rg}(2\lambda_{P,3} - 3\lambda_{P,2} + \lambda_{P,1})\lambda_{Q,0} + 2k_{rg}(\lambda_{P,2} - \lambda_{P,1})\}$$

Polymeric species R_n:

$$\frac{d\lambda_{R,0}}{dt} = \frac{N}{V^2}\{-2(2k_iG + k_tC_{P0})\lambda_{R,0} - k_1(\lambda_{R,1} - \lambda_{R,0}) + (C_{40} + \tfrac{1}{2}k_p\lambda_{Q,0})\lambda_{Q,0}\}$$

$$\frac{d\lambda_{R,1}}{dt} = \frac{N}{V^2}\{-2(2k_iG + k_tC_{P0})\lambda_{R,1} - k_1(\lambda_{R,2} - \lambda_{R,1}) + (C_{41} + \tfrac{1}{2}k_p\lambda_{Q,1})\lambda_{Q,0} + (C_{40} + \tfrac{1}{2}k_p\lambda_{Q,0})\lambda_{Q,1}\}$$

$$\frac{d\lambda_{R,2}}{dt} = \frac{N}{V^2}\{-2(2k_iG + k_tC_{P0})\lambda_{R,2} - k_1(\lambda_{R,3} - \lambda_{R,2}) + (C_{42} + \tfrac{1}{2}k_p\lambda_{Q,2})\lambda_{Q,0} + 2(C_{41} + \tfrac{1}{2}k_p\lambda_{Q,1})\lambda_{Q,1} + (C_{40} + \tfrac{1}{2}k_p\lambda_{Q,0})\lambda_{Q,2}\}$$

Polymeric species S_n:

$$\frac{d\lambda_{S,0}}{dt} = \frac{N}{V^2}\{2G(k_i\lambda_{U,0} + 2k_{eg}\lambda_{Y,0}) + 2k_3\lambda_{P,0} - (k_5 + 2k_{eg}G + k_eC_{P0})\lambda_{S,0} - k_1(\lambda_{S,1} - \lambda_{S,0}) + C_{10}\lambda_{S,0} + 2(C_{20} - k_p\lambda_{S,0})\lambda_{P,0} + (k_2 + k_4)(C_{E1} - C_{E0})\}$$

$$\frac{d\lambda_{S,1}}{dt} = \frac{N}{V^2}\{2G(k_i\lambda_{U,1} + 2k_{eg}\lambda_{Y,1}) + 2k_3\lambda_{P,1} - (k_5 + 2k_{eg}G + k_eC_{P0})\lambda_{S,1}$$
$$- (k_1 + 2k_{rg}\lambda_{P,0})(\lambda_{S,2} - \lambda_{S,1}) + C_{11}\lambda_{S,0} + C_{10}\lambda_{S,1} + 2(C_{21} - k_p\lambda_{S,1})\lambda_{P,0}$$
$$+ 2(C_{20} - k_p\lambda_{S,0})\lambda_{P,1} + \tfrac{1}{2}(k_2 + k_4)(C_{E2} - C_{E1}) + k_{rg}(\lambda_{P,2} - \lambda_{P,1})\lambda_{S,0}\}$$

$$\frac{d\lambda_{S,2}}{dt} = \frac{N}{V^2}\{2G(k_i\lambda_{U,2} + 2k_{eg}\lambda_{Y,2}) + 2k_3\lambda_{P,2} - (k_5 + 2k_{eg}G + k_eC_{P0})\lambda_{S,2}$$
$$- (k_1 + 4k_{rg}\lambda_{P,0})(\lambda_{S,3} - \lambda_{S,2}) + C_{12}\lambda_{S,0} + 2C_{11}\lambda_{S,1} + C_{10}\lambda_{S,2} + 2(C_{22} - k_p\lambda_{S,2})\lambda_{P,0}$$
$$+ 4(C_{21} - k_p\lambda_{S,1})\lambda_{P,1} + 2(C_{20} - k_p\lambda_{S,0})\lambda_{P,2} + \tfrac{1}{6}(k_2 + k_4)(2C_{E3} - 3C_{E2} + C_{E1})$$
$$+ \tfrac{2}{3}k_{rg}(2\lambda_{S,3} - 3\lambda_{S,2} + \lambda_{S,1})\lambda_{P,0} + \tfrac{1}{3}k_{rg}(2\lambda_{P,3} - 3\lambda_{P,2} + \lambda_{P,1})\lambda_{S,0} + 2k_{rg}(\lambda_{P,2} - \lambda_{P,1})\lambda_{S,1}\}$$

Polymeric species T_n:

$$\frac{d\lambda_{T,0}}{dt} = \frac{N}{V^2}\{2G(k_i\lambda_{V,0} + k_{eg}\lambda_{W,0}) + 2k_dC_{P0}\lambda_{P,0} - (k_5 + k_{pd}C_{P0})\lambda_{T,0} - k_1(\lambda_{T,1} - \lambda_{T,0})$$
$$+ C_{10}\lambda_{T,0} + 2(C_{30} - k_p\lambda_{T,0})\lambda_{P,0} + (k_2 + k_4)(C_{D1} - C_{D0})\}$$

$$\frac{d\lambda_{T,1}}{dt} = \frac{N}{V^2}\{2G(k_i\lambda_{V,1} + k_{eg}\lambda_{W,1}) + 2k_dC_{P0}\lambda_{P,1} - (k_5 + k_{pd}C_{P0})\lambda_{T,1} - (k_1 + 2k_{rg}\lambda_{P,0})(\lambda_{T,2} - \lambda_{T,1})$$
$$+ C_{11}\lambda_{T,0} + C_{10}\lambda_{T,1} + 2(C_{31} - k_p\lambda_{T,1})\lambda_{P,0} + 2(C_{30} - k_p\lambda_{T,0})\lambda_{P,1}$$
$$+ \tfrac{1}{2}(k_2 + k_4)(C_{D2} - C_{D1}) + k_{rg}(\lambda_{P,2} - \lambda_{P,1})\lambda_{T,0}$$

$$\frac{d\lambda_{T,2}}{dt} = \frac{N}{V^2}\{2G(k_i\lambda_{V,2} + k_{eg}\lambda_{W,2}) + 2k_dC_{P0}\lambda_{P,2} - (k_5 + k_{pd}C_{P0})\lambda_{T,2} - (k_1 + 4k_{rg}\lambda_{P,0})(\lambda_{T,3} - \lambda_{T,2})$$
$$+ C_{12}\lambda_{T,0} + 2C_{11}\lambda_{T,1} + C_{10}\lambda_{T,2} + 2(C_{32} - k_p\lambda_{T,2})\lambda_{P,0} + 4(C_{31} - k_p\lambda_{T,1})\lambda_{P,1}$$
$$+ 2(C_{30} - k_p\lambda_{T,0})\lambda_{P,2} + \tfrac{1}{6}(k_2 + k_4)(2C_{D3} - 3C_{D2} + C_{D1}) + \tfrac{2}{3}k_{rg}(2\lambda_{T,3} - 3\lambda_{T,2} + \lambda_{T,1})\lambda_{P,0}$$
$$+ \tfrac{1}{3}k_{rg}(2\lambda_{P,3} - 3\lambda_{P,2} + \lambda_{P,1})\lambda_{T,0} + 2k_{rg}(\lambda_{P,2} - \lambda_{P,1})\lambda_{T,1}\}$$

Polymeric species U_n:

$$\frac{d\lambda_{U,0}}{dt} = \frac{N}{V^2}\{k_3\lambda_{Q,0} - [2(k_i + k_{eg})G + (k_t + k_e)C_{P0}]\lambda_{U,1}$$
$$- k_1(\lambda_{U,1} - \lambda_{U,0}) + C_{20}\lambda_{Q,0} + C_{40}\lambda_{S,0} + k_4(C_{T1} - C_{T0})\}$$

$$\frac{d\lambda_{U,1}}{dt} = \frac{N}{V^2}\{k_3\lambda_{Q,1} - [2(k_i + k_{eg})G + (k_t + k_e)C_{P0}]\lambda_{U,1} - k_1(\lambda_{U,2} - \lambda_{U,1})$$
$$+ C_{21}\lambda_{Q,0} + C_{20}\lambda_{Q,1} + C_{41}\lambda_{S,0} + C_{40}\lambda_{S,1} + \tfrac{1}{2}k_4(C_{T2} - C_{T1})\}$$

$$\frac{d\lambda_{U,2}}{dt} = \frac{N}{V^2}\{k_3\lambda_{Q,2} - [2(k_i + k_{eg})G + (k_t + k_e)C_{P0}]\lambda_{U,2} - k_1(\lambda_{U,3} - \lambda_{U,2}) + C_{22}\lambda_{Q,0}$$
$$+ 2C_{21}\lambda_{Q,1} + C_{20}\lambda_{Q,2} + C_{42}\lambda_{S,0} + 2C_{41}\lambda_{S,1} + C_{40}\lambda_{S,2} + \tfrac{1}{6}k_4(2C_{T3} - 3C_{T2} + C_{T1})\}$$

Polymeric species V_n:

$$\frac{d\lambda_{V,0}}{dt} = \frac{N}{V^2}\{k_dC_{P0}\lambda_{Q,0} - [2k_iG + (k_t + k_{pd})C_{P0}]\lambda_{V,0} - k_1(\lambda_{V,1} - \lambda_{V,0})$$
$$+ C_{30}\lambda_{Q,0} + C_{40}\lambda_{T,0} + 2k'_{pd}D(C_{T1} - C_{T0})\}$$

$$\frac{d\lambda_{V,1}}{dt} = \frac{N}{V^2}\{k_d C_{P0}\lambda_{Q,1} - [2k_i G + (k_t + k_{pd})C_{P0}]\lambda_{V,1} - k_1(\lambda_{V,2} - \lambda_{V,1}) + C_{31}\lambda_{Q,0} + C_{30}\lambda_{Q,1} + C_{41}\lambda_{T,0} + C_{40}\lambda_{T,1} + k'_{pd}D(C_{T2} - C_{T1})\}$$

$$\frac{d\lambda_{V,2}}{dt} = \frac{N}{V^2}\{k_d C_{P0}\lambda_{Q,2} - [2k_i G + (k_t + k_{pd})C_{P0}]\lambda_{V,2} - k_1(\lambda_{V,3} - \lambda_{V,2}) + C_{32}\lambda_{Q,0} + 2C_{31}\lambda_{Q,1} + C_{30}\lambda_{Q,2} + C_{42}\lambda_{T,0} + 2C_{41}\lambda_{T,1} + C_{40}\lambda_{T,2} + \tfrac{1}{3}k'_{pd}D(2C_{T3} - 3C_{T2} - C_{T1})\}$$

Polymeric species W_n:

$$\frac{d\lambda_{W,0}}{dt} = \frac{N}{V^2}\{k_d C_{P0}\lambda_{S,0} + k_3\lambda_{T,0} - [2k_{eg}G + (k_t + k_{pd})C_{P0}]\lambda_{W,0} - k_1(\lambda_{W,1} - \lambda_{W,0}) + C_{30}\lambda_{S,0} + (C_{20} - k_p\lambda_{S,0})\lambda_{T,0} + k_4(C_{D1} - C_{D0}) + 2k'_{pd}D(C_{E1} - C_{E0})\}$$

$$\frac{d\lambda_{W,1}}{dt} = \frac{N}{V^2}\{k_d C_{P0}\lambda_{S,1} + k_3\lambda_{T,1} - [2k_{eg}G + (k_t + k_{pd})C_{P0}]\lambda_{W,1} - k_1(\lambda_{W,2} - \lambda_{W,1}) + C_{31}\lambda_{S,0} + C_{30}\lambda_{S,1} + (C_{21} - k_p\lambda_{S,1})\lambda_{T,0} + (C_{20} - k_p\lambda_{S,0})\lambda_{T,1} + \tfrac{1}{2}k_4(C_{D2} - C_{D1}) + k'_{pd}D(C_{E2} - C_{E1})\}$$

$$\frac{d\lambda_{W,2}}{dt} = \frac{N}{V^2}\{k_d C_{P0}\lambda_{S,2} + k_3\lambda_{T,2} - [2k_{eg}G + (k_t + k_{pd})C_{P0}]\lambda_{W,2} - k_1(\lambda_{W,3} - \lambda_{W,2}) + C_{32}\lambda_{S,0} + 2C_{31}\lambda_{S,1} + C_{30}\lambda_{S,2} + (C_{22} - k_p\lambda_{S,2})\lambda_{T,0} + 2(C_{21} - k_p\lambda_{S,1})\lambda_{T,1} + (C_{20} - k_p\lambda_{S,0})\lambda_{T,2} + \tfrac{1}{6}k_4(2C_{D3} - 3C_{D2} + C_{D1}) + \tfrac{1}{3}k'_{pd}D(2C_{E3} - 3C_{E2} + C_{E1})\}$$

Polymeric species Y_n:

$$\frac{d\lambda_{Y,0}}{dt} = \frac{N}{V^2}\{k_3\lambda_{S,0} - 2(2k_{eg}G + k_e C_{P0})\lambda_{Y,0} - k_1(\lambda_{Y,1} - \lambda_{Y,0}) + (C_{20} - \tfrac{1}{2}k_p\lambda_{S,0})\lambda_{S,0} + k_4(C_{E1} - C_{E0})\}$$

$$\frac{d\lambda_{Y,1}}{dt} = \frac{N}{V^2}\{k_3\lambda_{S,1} - 2(2k_{eg}G + k_e C_{P0})\lambda_{Y,1} - k_1(\lambda_{Y,2} - \lambda_{Y,1}) + (C_{21} - \tfrac{1}{2}k_p\lambda_{S,1})\lambda_{S,0} + (C_{20} - \tfrac{1}{2}k_p\lambda_{S,0})\lambda_{S,1} + \tfrac{1}{2}k_4(C_{E2} - C_{E1})\}$$

$$\frac{d\lambda_{Y,2}}{dt} = \frac{N}{V^2}\{k_3\lambda_{S,2} - 2(2k_{eg}G + k_e C_{P0})\lambda_{Y,2} - k_1(\lambda_{Y,3} - \lambda_{Y,2}) + (C_{22} - \tfrac{1}{2}k_p\lambda_{S,2})\lambda_{S,0} + (C_{21} - \tfrac{1}{2}k_p\lambda_{S,1})\lambda_{S,0} + (C_{20} - \tfrac{1}{2}k_p\lambda_{S,0})\lambda_{S,1} + \tfrac{1}{6}k_4(2C_{E3} - 3C_{E2} + C_{E1})\}$$

Polymeric species Z_n:

$$\frac{d\lambda_{Z,0}}{dt} = \frac{N}{V^2}\{k_d C_{P0}\lambda_{T,0} - 2k_{pd}\lambda_{Z,0} - k_1(\lambda_{Z,1} - \lambda_{Z,0}) + (C_{30} - \tfrac{1}{2}k_p\lambda_{T,0})\lambda_{T,0} + 2k'_{pd}D(C_{D1} - C_{D0})\}$$

$$\frac{d\lambda_{Z,1}}{dt} = \frac{N}{V^2}\{k_d C_{P0}\lambda_{T,1} - 2k_{pd}\lambda_{Z,1} - k_1(\lambda_{Z,2} - \lambda_{Z,1}) + (C_{31} - \tfrac{1}{2}k_p\lambda_{T,1})\lambda_{T,0} + (C_{30} - \tfrac{1}{2}k_p\lambda_{T,0})\lambda_{T,0} + k'_{pd}D(C_{D2} - C_{D1})\}$$

$$\frac{d\lambda_{Z,2}}{dt} = \frac{N}{V^2}\{k_d C_{P0}\lambda_{T,2} - 2k_{pd}\lambda_{Z,2} - k_1(\lambda_{Z,3} - \lambda_{Z,2}) + (C_{32} - \tfrac{1}{2}k_p\lambda_{T,2})\lambda_{T,0} + 2(C_{31} - \tfrac{1}{2}k_p\lambda_{T,1})\lambda_{T,1} + (C_{30} - \tfrac{1}{2}k_p\lambda_{T,0})\lambda_{T,2} + \tfrac{1}{3}k'_{pd}D(2C_{D3} - 3C_{D2} + C_{D1})\}$$

where

$$C_{P0} = 2\lambda_{P,0} + \lambda_{Q,0} + \lambda_{S,0} + \lambda_{T,0}$$

$$C_{P1} = 2\lambda_{P,1} + \lambda_{Q,1} + \lambda_{S,1} + \lambda_{T,1}$$

$$C_{P2} = 2\lambda_{P,2} + \lambda_{Q,2} + \lambda_{S,2} + \lambda_{T,2}$$

$$C_{P3} = 2\lambda_{P,3} + \lambda_{Q,3} + \lambda_{S,3} + \lambda_{T,3}$$

$$C_{T0} = \lambda_{Q,0} + 2\lambda_{R,0} + \lambda_{U,0} + \lambda_{V,0}$$

$$C_{T1} = \lambda_{Q,1} + 2\lambda_{R,1} + \lambda_{U,1} + \lambda_{V,1}$$

$$C_{T2} = \lambda_{Q,2} + 2\lambda_{R,2} + \lambda_{U,2} + \lambda_{V,2}$$

$$C_{T3} = \lambda_{Q,3} + 2\lambda_{R,3} + \lambda_{U,3} + \lambda_{V,3}$$

$$C_{E0} = \lambda_{S,0} + \lambda_{U,0} + \lambda_{W,0} + 2\lambda_{Y,0}$$

$$C_{E1} = \lambda_{S,1} + \lambda_{U,1} + \lambda_{W,1} + 2\lambda_{Y,1}$$

$$C_{E2} = \lambda_{S,2} + \lambda_{U,2} + \lambda_{W,2} + 2\lambda_{Y,2}$$

$$C_{E3} = \lambda_{S,3} + \lambda_{U,3} + \lambda_{W,3} + 2\lambda_{Y,3}$$

$$C_{D0} = \lambda_{T,0} + \lambda_{V,0} + \lambda_{W,0} + 2\lambda_{Z,0}$$

$$C_{D1} = \lambda_{T,1} + \lambda_{V,1} + \lambda_{W,1} + 2\lambda_{Z,1}$$

$$C_{D2} = \lambda_{T,2} + \lambda_{V,2} + \lambda_{W,2} + 2\lambda_{Z,2}$$

$$C_{D3} = \lambda_{T,3} + \lambda_{V,3} + \lambda_{W,3} + 2\lambda_{Z,3}$$

$$C_{10} = 2k_p\lambda_{P,0} + k_t\lambda_{Q,0} + k_e\lambda_{S,0} + k_{pd}\lambda_{T,0}$$

$$C_{11} = 2k_p\lambda_{P,1} + k_t\lambda_{Q,1} + k_e\lambda_{S,1} + k_{pd}\lambda_{T,1}$$

$$C_{12} = 2k_p\lambda_{P,2} + k_t\lambda_{Q,2} + k_e\lambda_{S,2} + k_{pd}\lambda_{T,2}$$

$$C_{20} = k_p\lambda_{S,0} + k_t\lambda_{U,0} + k_{pd}\lambda_{W,0} + 2k_e\lambda_{Y,0}$$

$$C_{21} = k_p\lambda_{S,1} + k_t\lambda_{U,1} + k_{pd}\lambda_{W,1} + 2k_e\lambda_{Y,1}$$

$$C_{22} = k_p\lambda_{S,2} + k_t\lambda_{U,2} + k_{pd}\lambda_{W,2} + 2k_e\lambda_{Y,2}$$

$$C_{30} = k_p\lambda_{T,0} + k_t\lambda_{V,0} + k_e\lambda_{W,0} + 2k_{pd}\lambda_{Z,0}$$

$$C_{31} = k_p\lambda_{T,1} + k_t\lambda_{V,1} + k_e\lambda_{W,1} + 2k_{pd}\lambda_{Z,1}$$

$$C_{32} = k_p\lambda_{T,2} + k_t\lambda_{V,2} + k_e\lambda_{W,2} + 2k_{pd}\lambda_{Z,2}$$

$$C_{40} = 2k_t\lambda_{R,0} + k_e\lambda_{U,0} + k_{pd}\lambda_{V,0}$$

$$C_{41} = 2k_t\lambda_{R,1} + k_e\lambda_{U,1} + k_{pd}\lambda_{V,1}$$

$$C_{42} = 2k_t\lambda_{R,2} + k_e\lambda_{U,2} + k_{pd}\lambda_{V,2}$$

References

1. K. Ravindranath and R. A. Mashelkar, *Chem. Eng. Sci.*, **41**(9), 2197–2214 (1986).
2. K. Ravindranath and R. A. Mashelkar, *Chem. Eng. Sci.*, **41**(12), 2969–2987 (1986).
3. J.-M. Besnoin and K. Y. Choi, *J. Macromol. Sci. Rev. Macromol. Chem. Phys.*, **29**(1), 55 (1989).

4. K. Ravindranath and R. A. Mashelkar, *J. Appl. Polym. Sci.*, **27**, 2625–2652 (1982).
5. K. Ravindranath and R. A. Mashelkar, *Polym. Eng. Sci.*, **22**(10), 619–627 (1982).
6. K. Ravindranath and R. A. Mashelkar, *Polym. Eng. Sci.*, **22**(10), 628–636 (1982).
7. K. Ravindranath and R. A. Mashelkar, *Polym. Eng. Sci.*, **24**(1), 30–41 (1984).
8. A. Kumar, S. K. Gupta, B. Gupta, and D. Kunzru, *J. Appl. Polym. Sci.*, **27**, 4421–4438 (1982).
9. A. Kumar, S. K. Gupta and N. Somu, *Polym. Eng. Sci.*, **22**(5), 314–323 (1982).
10. A. Kumar, S. K. Gupta, S. Madan, N. G. Shah, and S. K. Gupta, *Polym. Eng. Sci.*, **24**(3), 194–204 (1984).
11. A. Kumar, S. N. Sharma, and S. K. Gupta, *J. Appl. Polym. Sci.*, **29**, 1045–1061 (1984).
12. W. S. Ha and Y. K. Choun, *J. Polym. Sci. Polym. Chem. Ed.*, **17**, 2103 (1979).
13. D. A. S. Ravens and I. M. Ward, *Trans. Faraday. Soc.*, **57**, 150 (1961).
14. K. Yoda, *Kobunshi Kagaku*, **24**, 472–478 (1967).
15. K. Tomita, *Polymer*, **14**, 50–54 (1973).
16. K. Tomita, *Polymer*, **17**, 221–224 (1976).
17. H. Yokoyama, T. Sano, T. Chijiiwa, and R. Kajiya, *J. Jpn. Petrol. Inst.*, **21**(1), 58–62 (1978).
18. K. Ravindranath and R. A. Mashelkar, *J. Appl. Polym. Sci.*, **26**, 3179–3204 (1981).
19. J. M. Prausnitz, *Molecular Thermodynamics of Fluid-Phase Equilibria*, Prentice-Hall, Englewood Cliffs, NJ, 1969.
20. S. K. Gupta, D. Mohan, and A. Kumar, *J. Appl. Polym. Sci.*, **30**, 445–460 (1985).
21. J. W. Ault and D. A. Mellichamp, *Chem. Eng. Sci.*, **27**, 2219 (1972).
22. H. Yokoyama, T. Sano, T. Chijiiwa, and R. Kajiya, *J. Jpn. Petrol. Inst.*, **21**(3), 194–198 (1978).
23. J.-M. Besnoin, M.S. thesis, University of Maryland, 1988.
24. G. S. Kirshenbaum, W. T. Freed, M. W. Dong, and J. T. Carano, *Org. Coat. Plast. Chem.*, **41**, 324 (1979).
25. F. F. Leigner, *Org. Coat. Plast. Chem.*, **41**, 330 (1979).
26. E. P. Goodings, *Soc. Chem. Ind. (London)*, Monograph No. 13, 211 (1961).

Received January 23, 1989
Accepted March 20, 1990